NUREG/CR-3263
SAND83-2622
RV
Printed April 1984

LA GRANGE

Status Report: Correlation of Electrical Cable Failure With Mechanical Degradation

Otmar Stuetzer

Prepared by
Sandia National Laboratories
Albuquerque, New Mexico 87185 and Livermore, California 94550
for the United States Department of Energy
under Contract DE-AC04-76DP00789

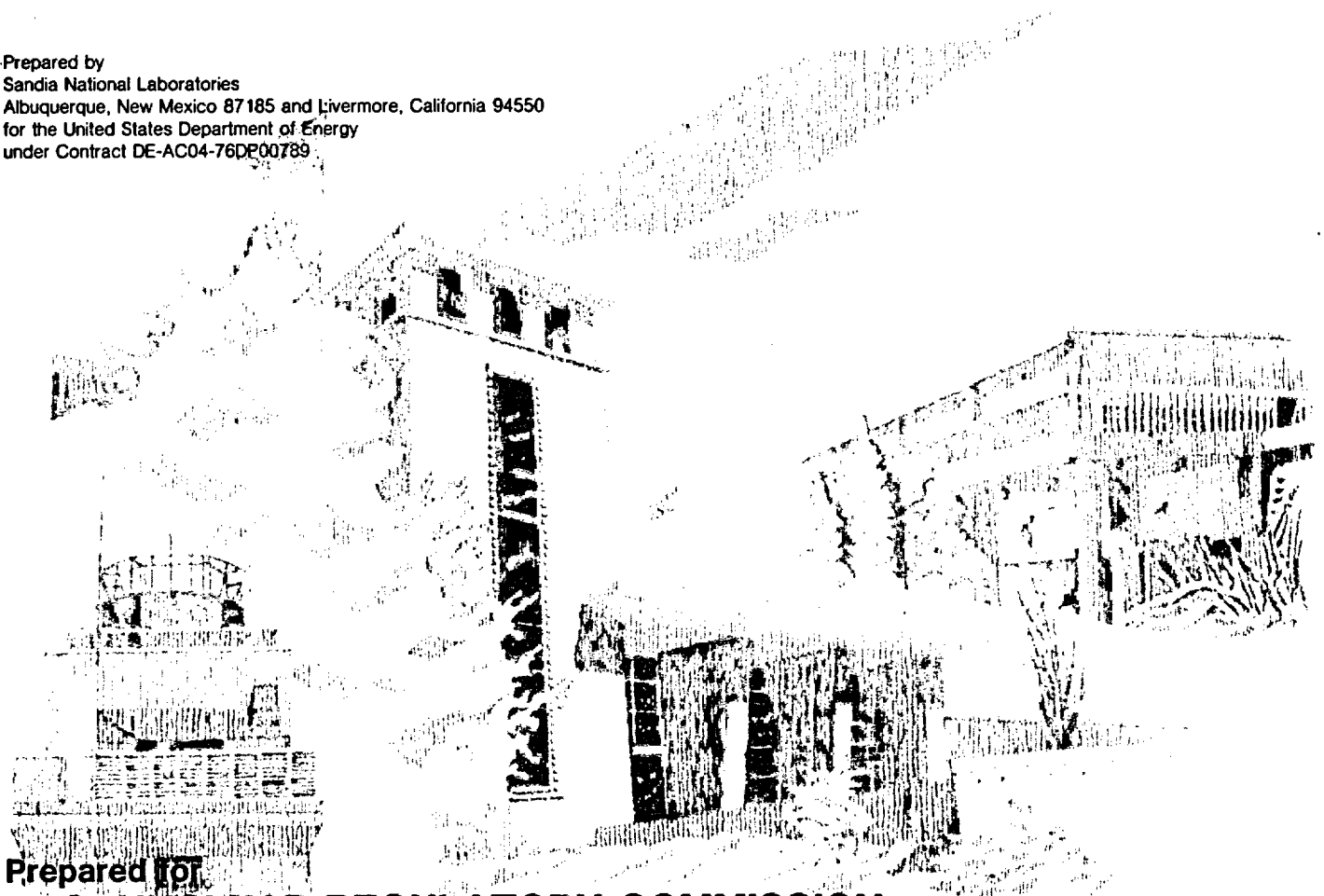

Prepared for
U. S. NUCLEAR REGULATORY COMMISSION

SF2900Q (8-81)

Available from

GPO Sales Program
Division of Technical Information and Document Control
U.S. Nuclear Regulatory Commission
Washington, D.C. 20555

and

National Technical Information Service
Springfield, Virginia 22161

NUREG/CR-3263
SAND83-2622
RV

STATUS REPORT: CORRELATION OF ELECTRICAL CABLE FAILURE WITH MECHANICAL DEGRADATION

Otmar Stuetzer

Printed: April 1984

Sandia National Laboratories
Albuquerque, NM 87185
Operated by
Sandia Corporation
for the
U.S. Department of Energy

Prepared for

Office of Nuclear Regulatory Research
U.S. Nuclear Regulatory Commission
Washington, DC 20555
Under Memorandum of Understanding DOE 40-550-75
NRC FIN No. A-1051

ABSTRACT

An attempt is being made to assess complete electrical failure of signal and low-power cables typically used in nuclear power plant containments and to correlate failure modes with the mechanical deterioration of the elastomeric cable material. Work over the past 24 months, although limited to one cable configuration, has identified creep shortout and insulator cracking, both aggravated by mechanical stresses, as the phenomena most likely to cause electrical breakdown. Comprehensive tests have been run for six months and are continuing. Preliminary conclusions can be drawn and are reported.

CONTENTS

ILLUSTRATIONS

ILLUSTRATIONS (cont.)

LIST OF TABLES

ACKNOWLEDGMENTS

The project was initiated and has been monitored by L. L. Bonzon, who provided essential administrative support and continuous technical guidance. Discussions with K. T. Gillen and L. D. Bustard were helpful. D. G. Sample assisted in the design of the X-ray measurement system and assumed responsibility for development and accurate magnification of the pictures. B. D. Haensche investigated suitable image evaluation methods and provided digitized magnifications with density traces.

Particular acknowledgment is due to G. J. Simmons, who designed and built all special instruments and mechanical devices, designed and installed the test facility, and made most of the measurements.

EXECUTIVE SUMMARY

The purpose of this investigation is to link the degradation of the elastomeric cable materials with the actual potential for circuit failure of safety-related cables in the containment building of a nuclear power plant; failure is defined as an electrical shortout or as an obvious shortout path.

In the introduction (Section I), the essential difficulties and limitations of the present work are discussed. A very large number of independent variables (e.g., composition, geometry, additives, aging sequences, rate effects) lead to a high degree of complexity and force judicious constraints on experimentation. Further complications are introduced by the shortcomings of accelerated testing methods. Single-conductor, 480 V, power cables with ethylene propylene rubber (EPR) insulators and Hypalon jacket were chosen for the experiments. With this configuration, a number of experiments large enough to be statistically significant are feasible. This approach furnishes sufficient data to form a base for extrapolation by means of scaling models to other geometries and to other mechanical boundary conditions.

Literature data and several hundred scoping tests (Section II) are the basis for a discussion of purely electrical failures; i.e. failures occurring when cables are not mechanically stressed or handled. It is shown that direct electrical-field breakdown as well as thermal runaway is very unlikely at rated voltages even after long-term exposure to high temperatures (190°C) and to high total doses of gamma radiation (10^8 rads); rate effects are negligible or perhaps even beneficial. The deterioration of insulation resistance due to the presence of strong continuous radiation (10 Mrad/h), during an accident, leads to only negligibly small shunt currents; also, high humidity has little influence in the absence of cracks. Thus, it is concluded that cables exposed to the environment in a reactor containment for 40 years, but undisturbed and unstressed, are highly unlikely to fail. This fact simplifies the present investigation by limiting it to situations where the geometry of the cable is affected by mechanical forces.

The remaining failure mechanisms fall into two categories. First, if the cable is stretched by an applied force (or by its own weight) over an edge with small curvature, the metal wires will gradually creep through the soft polymeric insulation resulting in metallic contact between cable wires or a wire and the cable support, shorting the cable (creep shortout). Second, the polymeric materials embrittled by aging may crack under mechanical stress. To permit long-term aging, creep, and cracking measurements, a dedicated facility (Section III) has been established. It consists principally of seven temperature-controlled heat chambers, in which stressed and unstressed cable samples are exposed to constant elevated

temperatures for long periods. Creep distances can be precision measured by X-raying at regular intervals.

Systematic creep experiments (Section IV) are presently performed on cable samples that are bent in a U-shape over a 4.8-mm diameter support rod with each cable end supporting a 1-lb weight. After 7 months, no situation approaching short-out has been identified. It was found that the most severe creep deformation occurred at a temperature of approximately 125°C. Apparently, at higher temperatures, polymer embrittlement proceeds so fast that it effectively inhibits creep.

For the investigation of crack failures (Section V), it is stipulated that any crack penetrating to the metal wire constitutes cable failure. Three specific situations are being investigated:

a) Long cables (10 m or more), lying undisturbed in conduits, may develop cracks under thermal cycling. So far, this phenomenon has only been observed when the cable temperature exceeded 150°C.

b) Cables that are sharply bent may develop cracks under mechanical stresses caused by thermal cycling or by weighting. Severe cracking tends to occur at temperatures above 175°C.

c) Cables embrittled by aging may be stressed and cracked during maintenance activities. A simple model links the onset of cracks to the bending radius and the breaking strain at elongation for the cable materials. Experimental results show good correlation with the model.

During the investigations, phenomena were observed that tend to decrease the failure probability of cables. For example, in bent and stressed specimens, the polymeric material becomes more dense above the support area, which improves the breakdown field strength of the material. In addition there is a worst position for the lie of the strands in the conductor, this position leading to maximum creep. One moderating factor, though, is that this position is mechanically unstable and tends to eliminate itself.

While the investigation is still proceeding, a number of conclusions (Section VI) may already be drawn. Cables are basically very reliable components with very low failure probability. Failures are mostly due to marginal design or handling practices. Operational integrity for EPR - Hypalon power cables is predicted under the following conditions:

(1) The cable temperature does not exceed 190°C (thermal runaway condition), and exposure time at high temperatures is limited, so cracks in unstressed cables do not occur.

(2) Cable overhang over edges with small radius of curvature does not exceed 10 m (creep shortout condition).

(3) Cables for which the breaking strain ratio (elongation-at-break ratio) has become less than 0.4 are not handled or permitted to move mechanically (bending crack condition).

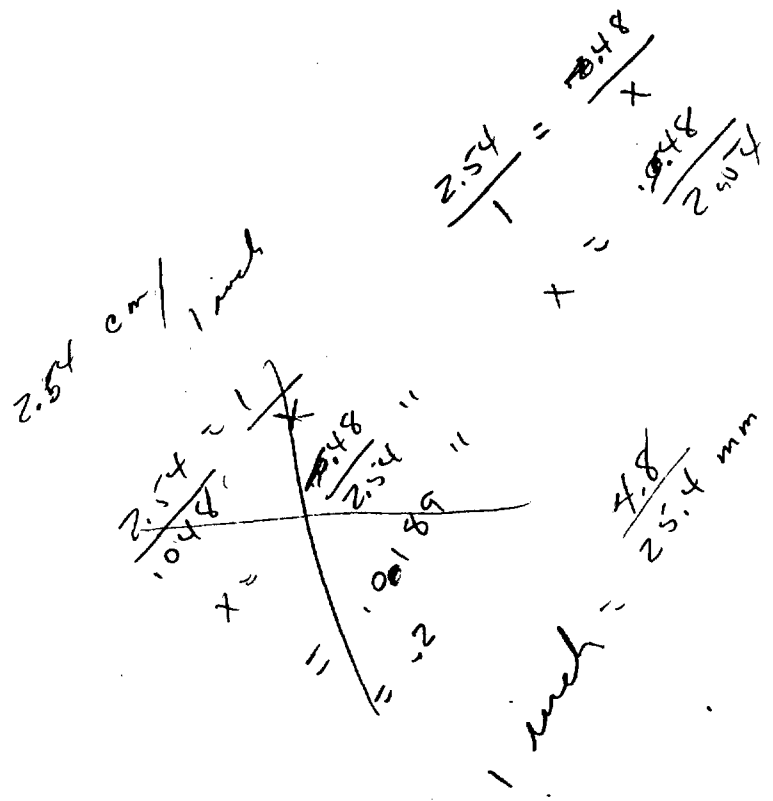

I. INTRODUCTION

Improvement in the understanding of the complex aging and deterioration behavior of elastomeric cable materials exposed to the environment in the containment of a nuclear power plant is continuing. However, the correlation of observed material changes with the electrical failure rate of the cable circuit has not yet been achieved. This problem is of considerable complexity due to the large number of variables introduced by materials combinations, additives, rate effects, circuitry, aging sequences, environments, mechanical support, and others. Even a conservative compilation (c.f., Appendix A) shows from 25 to 30 independent parameters leading to hundreds of thousands of different combinations. The situation is further aggravated by two additional facts:

(1) Cables, per se, are simple and well-developed components, whose failure rate is very low; many experiments are therefore needed to determine reasonably reliable and statistically valid failure data, and

(2) Many parameters of possible importance, such as additives and materials processing sequences, are proprietary, often unknown, and/or batch variable; this requires a multiplicity of tests for statistical evaluation.

Reasonable constraints had to be imposed to keep the investigation within feasible limits and achievable goals. Literature studies and several hundred scoping tests served to bound and define an acceptable program. The program's aim is to find and understand the most important operational failure mechanisms for electrical cables in a nuclear-reactor containment. Extrapolation to 40-yr exposure with the possibility of a reactor accident at the end of this time is desirable.

Considerable simplification is possible through the realization that for modern qualified cables operated at design voltages or less, the deterioration of most electrical properties of the cable (such as loss factor or breakdown field strength) is unlikely to lead to electrical-system failure even if combined (synergistic) effects are taken into account. Two electromechanical failure mechanisms are of concern, however: (1) creep shortout, occurring when a mechanically stressed cable is bent over a corner and conductors are pulled towards each other or towards a grounded electrode, and (2) cracking of the insulating layers, which in the presence of electrolytic conduction may lead to current diversion.

One constraint imposed on the program is the use of a single combination of materials (EPR for the insulating material and Hypalon for the jacket) and a single cable geometry (600 V, 20-A rated low-power cable); this cable type is typically used in nuclear-power plants. An attempt is being made to

generalize the results to other cable types by correlating the observed cable damage with the rather well-known materials deterioration. Analytical extrapolation to other geometries and to a variety of mechanical stresses is accomplished by correlation to, and then generalization from, simple scaling models. With this approach, it was feasible to limit the number of experiments to 84 temperature-time value pairs per year. The number of tests for each value pair (6 precision creep measurements and 40 crack tests) was chosen so that it is large enough to be statistically significant.

A number of additional simplifications are made, that are generally thought to be on the conservative side (i.e., increasing the predicted frequency of damage). First, for crack-caused electrical failure, any crack penetrating through the jacket to the cable insulator was assumed to be a "failure." Second, it was assumed that radiation exposure mitigates creep shortout by embrittling the polymers; hence, in the creep experiments, only temperature exposure is used as an aging mechanism. Third, to extrapolate cracking data, a working hypothesis was used that links cracking to the end value of the breaking strain for the materials, disregarding the combination of radiation and/or time-temperature exposures under which the breaking strain was obtained. Fourth, (and perhaps not necessarily conservative), creep shortout was defined as an impedance of less than some fraction of an ohm. These simplifications decrease the number of necessary experiments and allow a bounding of the problem.

To some degree these simplifications are compensated for by addition of test parameters. Up to now, maximum temperatures during an accident were generally considered to be below 165°C; for this investigation, maximum test-parameter temperatures of up to 225°C were included. The reasons are threefold: (1) an expectation that predicted containment temperatures may be increased to account for severe accident scenarios, (2) the fact that cables may be overloaded and therefore hotter than the environment, and (3) the desire to accelerate the aging process in experiments being conducted.

Further complication is introduced by the shortcomings of accelerated testing methods. Creep and cracking phenomena cannot be assumed to exhibit Arrhenius-type behavior. Extrapolations to 40 years may require measurements over many years, at least for situations where no physical arguments are readily available to establish the direction of long-term trends. For this reason, and to permit desirable proof tests, a dedicated long-term exposure facility has been established. It consists of seven automatically controlled heat chambers and three large heat pipes, all designed to operate with minimum attention for long periods. Self-calibrating fixtures that permit accurate mechanical measurements over long times have been incorporated.

In the following sections the essential details of the work performed to date will be described. In Section II, literature data and preliminary experiments will be discussed; it will be shown that purely electrical breakdown is unlikely for the cable type under consideration. In Section III, arrangements used to obtain creep and cracking data are described, together with calibration and correction methods. Section IV concerns creep measurements and the results of a first-order (two-dimensional) creep analysis. In Section V, the cracking data obtained are analyzed. Section VI summarizes the results and discusses possible and probable consequences.

II. PURELY ELECTRICAL FAILURES

Electrical cables used in nuclear power stations are very reliable components. An investigation[1] of 1400 reactor trips in 42 pressurized-water reactors between 1961 and 1978 lists only 8 shutdowns caused by cables; 5 of these failures were due to electrical shorts. An average of 7.2 outages per plant per year is found by the author; this leads to a 4% probability of a severe operational cable failure per plant per year. As there are typically 500-1500 km of cables in a reactor containment system,[2] the failure probability per meter of cable per year is very low (about 4×10^{-8}). For example, no accident occurred during the span of the above investigation, given that no cable failure has been proven for the Three Mile Island accident.[3] To simplify matters, no attempt is made to separate the type of failures in the above work.

The goal in this section is to attempt to show that purely electrical failures (complete field breakdown or thermal runaway melting the insulation) in cables exposed for 40 years to the environment in the containment of a nuclear power plant, and then to a design-basis accident, are highly unlikely. This assumes the cables are not handled or mechanically stressed. Medium voltage (approximately 500 volt) low-power cables, those normally considered the most likely to fail, are used, and it is assumed that the cables are operated within ratings; severe overloads due to circuit breaker failure are not included in the analysis. Insulating materials of interest are the ones used most often in modern reactor cabling (e.g., PE, XLPE, XLPO, and EPR, with Hypalon as a typical jacket material). The electrical properties of the various materials are quite similar; average breakdown field strengths differ by factors of 3, and conductivities by factors of 10 in either direction. For the purpose of this discussion, order of magnitude argumentation is justified; differences between insulator and jacket can then be ignored.

All cables are assumed to be qualified for nuclear power applications; i.e., test samples have been exposed to a simultaneous or sequential temperature and radiation treatment designed to simulate a 40-yr exposure to a typical reactor-containment environment; a design-basis accident simulation follows, during or after which the electrical quality of the cable is tested. The tests are not intended to yield and do not yield statistically meaningful reliability numbers, as the quantity of cable tested is small. Furthermore, the Arrhenius approximations used to extrapolate 40 years into the future are being challenged by some workers.[4] However, to avoid 40-yr tests, the qualification procedure involves radiation overexposure and electrical overtests. Experience supports the conclusion that the qualification procedure is meaningful. Few overall failures and fewer,

if any, purely electrical failures have occurred even in cables exposed to reactor-containment environment for long periods.[1,5]

More recently, it was confirmed that rate effects[6] and synergistic rate/temperature effects[7] can lead to unexpected mechanical deterioration in cable materials. The resulting impact on the important electrical properties of cables falls within the scope of the present investigation. It is also desirable to extend exposures to higher temperature than presently used in qualification procedures to encompass a greater temperature range and to reduce acceleration test times.[8] It will now be shown that the above effects do not influence breakdown properties and have a small and manageable influence on cable conductivity. It should be noted that the experiments discussed do not intentionally expose cables to mechanical stresses.

1. Field Breakdown

Qualification tests with high dose-rate aging have been reported by a number of investigators, including Bennet[9] (XLPO), Thome[10] (XLPE and EPR), and Hosticka et al.[11] (XLPE); all of whom used minor variations of the standard IEEE qualification method.[12] The tests revealed no breakdowns except when cables were cracked by rewinding and then immersed in water (the case excluded in this section).

Of particular interest is a report by Grüb and Langeset,[5] who exposed unusually long lengths of EPR cabling to a total of 300 Mrad of radiation (combined gammas, betas, and neutrons) over 4 years. The authors found no noticeable change in breakdown field strength over this time and dosage. The average dose rate in the Grüb-Langeset test was about 8 krad/h, much less than generally used for qualification aging. Dose-rate effects on the breakdown field strength of EPR, then, must be very low or negligible. The same conclusion is indicated by Figure 1, which shows dose-rate-effect measurements of Asaka.[13]

As was the case in Asaka's work, breakdown tests for cables are generally conducted at room temperature. Occasionally, tests are also conducted at the highest temperature predicted during an accident. For EPR, the breakdown field increases with increasing temperature, as Corbelli and Tonioli[14] have found for temperatures below 100°C. One possible explanation is that breakdown-causing gases diffuse outward more easily at higher temperatures. Measurements by St. Onge et al.,[15] compiled in Table 1, verify this dependence up to 170°C for EPR, while measurements for XLPE show a decline of the breakdown field to one-half as temperature increases to 170°C.

Extensive measurements of breakdown field strength above 170°C were performed during our investigations. An example for EPR

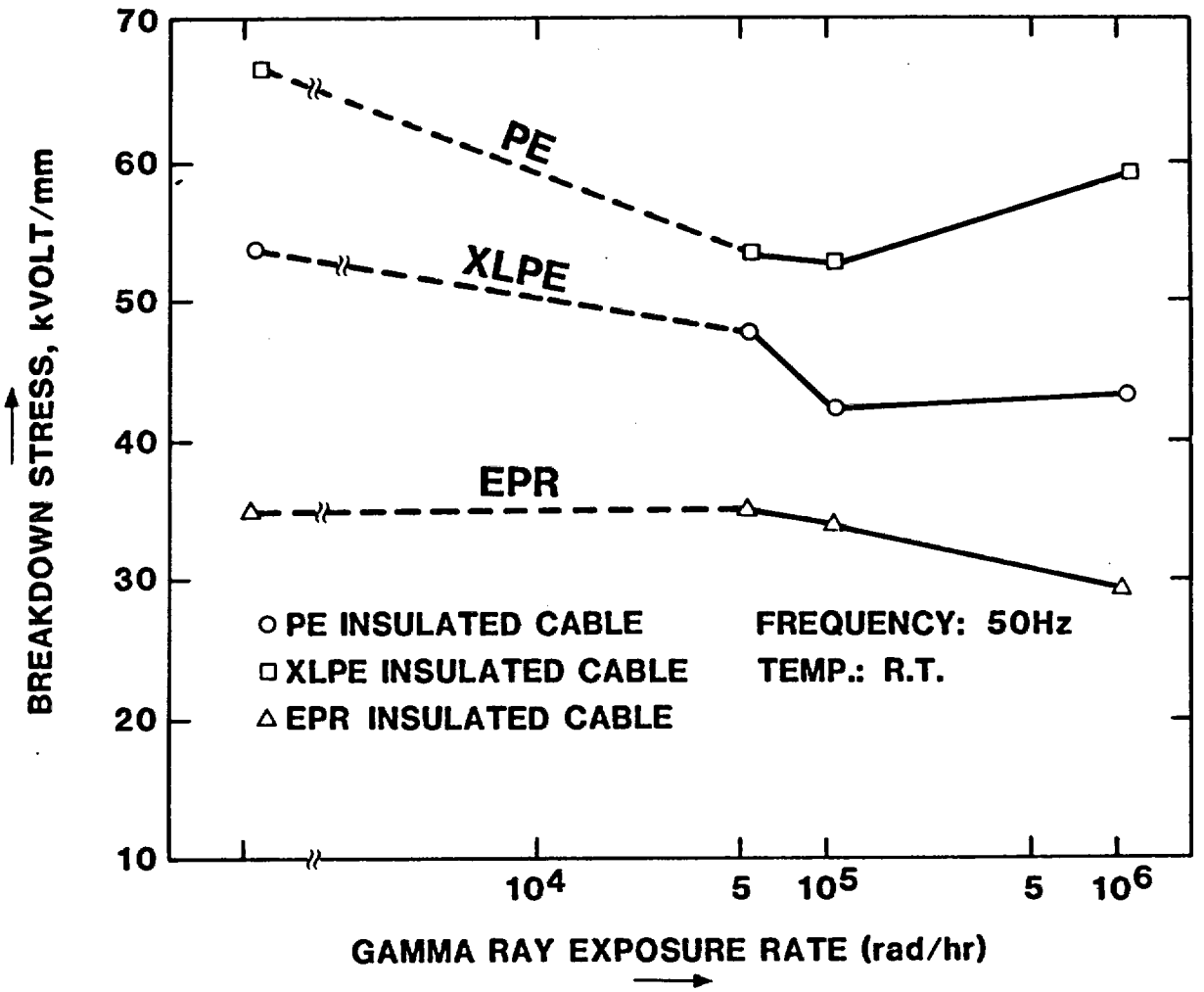

Figure 1. Dose-Rate Dependency of Breakdown Stress (After Asaka, Ref. 13)

Table 1

60 Hz Breakdown Field and Standard Deviation for Various Materials at Different Temperatures (After St. Onge, Ref. 15)

Materials	Breakdown field (standard deviation) (kV/mm) 23°C	60°C	90°C	110°C	130°C	150°C	170°C
XLPE, molded fully cured	74(6.7)	57(2.8)	47(3)	37(6.1)	36(6.2)	36(4.2)	39(6.6)
XLPE, molded partially cured	70(6.5)	66(3.0)	46(3.8)	39(4.8)	33(6.8)	26(4.6)	33(5.9)
XLPE, cable	66(7.9)	49(6.1)	42(3.2)	36(2.2)	40(1.9)	37(6.1)	30(5.5)
Filled XLPE	55(6.8)	59(1.3)	49(4.6)	49(4.9)	51(5.1)	50(4.1)	47(3.9)
EPR 1	41(7.4)	46(4.0)	46(1.3)	45(3.9)	51(2.4)	53(2.8)	50(2.7)
EPR 2	40(2.7)	44(2.2)	43(3.6)	44(3.7)	40(4.0)	45(3.8)	44(10.6)
EPR 3	36(4.6)	40(5.9)	38(6.9)	44(2.9)	45(2.3)	42(4.5)	40(2.5)
EPR 4	46(1.6)	47(2.7)	45(5.8)	50(1.7)	52(3.2)	49(2.8)	54(2.3)

is shown in Figure 2 for 225°C. It was noted that the average breakdown voltage increased about 10% over that observed for the room-temperature voltage, while the standard deviation stayed about the same.

It is concluded that increasing temperature and radiation rates do not severely decrease the breakdown field strength and, by increasing the breakdown strength, are sometimes beneficial. Synergistic effects are unlikely and apparently have never been reported.

2. Dielectric Loss Failure

A second purely electrical failure mechanism is caused by a strong increase in dielectric loss or insulator conductivity, which may lead to circuit starvation or to thermal runaway. Loss factor (for ac) and insulator resistivity (for dc) are related parameters used to assess the damage phenomena.

Dose-rate influences on the two parameters were measured by Kuriyama et al.[16] and are presented in Figure 3. There is only a small change in each parameter as the dose-rate increases. Seguchi et al.[17] have exposed EPR and low-density PE cables to irradiation with dose rates varying from 5 to 500 krad/h and to a total dose of 100 Mrad. The authors find there are no dose-rate effects if the materials contain anti-oxidants; otherwise, the dissipation factor increases by about 50% with decreasing dose rate, which is in agreement with Kuriyama's results. It is concluded that dose-rate effects are small and not important for dielectric losses.

In contrast, the influence of temperature on cable losses are substantial, although generally temporary (i.e., they last only as long as the temperature is elevated). In Figure 4, the insulation resistance as measured by Murata et al.[18] during a LOCA simulation is plotted. Compared to room temperature, temperatures of 174°C decrease resistivity by nearly 4 orders of magnitude. The data are only slightly affected by the aging methods used.

Figure 5 gives an example of higher temperature measurements (up to 225°C) performed in our investigation. The dc leakage current (I_L), averaged over ten 1-m-long cable samples, is seen to increase by nearly 7 orders of magnitude over the current measured at room temperature. The ac dissipation factor (D) first decreases with increasing temperature (as additives perhaps diffuse out of the polymers) and then rises to not quite 0.35; dissipation factors were measured at operational ac voltages and frequencies.

The following discussion of thermal runaway is based on a comparison of the heat generated by losses in the conductor of the cable and the additional heat caused by the dielectric losses in the insulator and the jacket. The first quantity

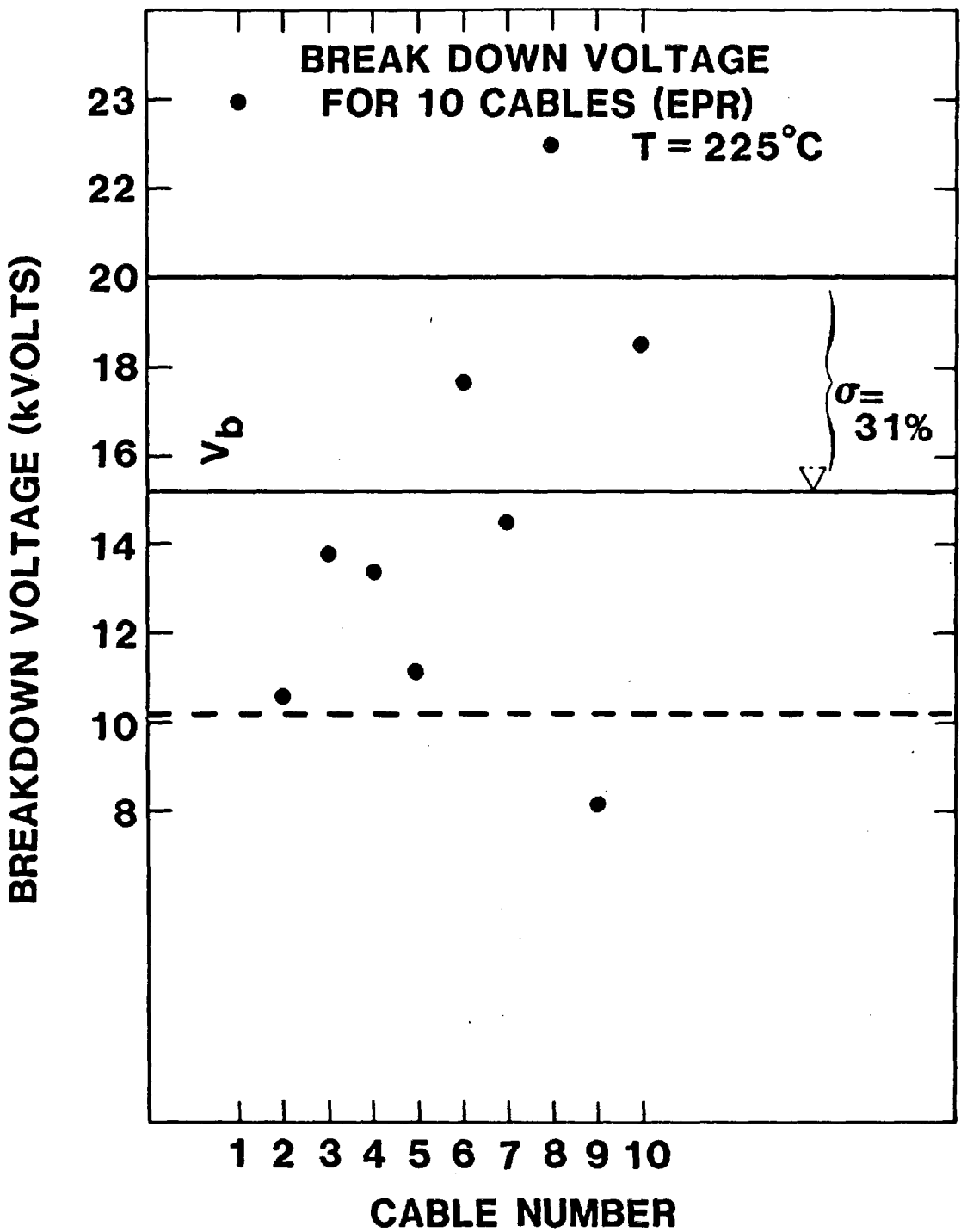

Figure 2. Breakdown Voltage (V_b) and Its Standard Deviation (σ) at 225°C

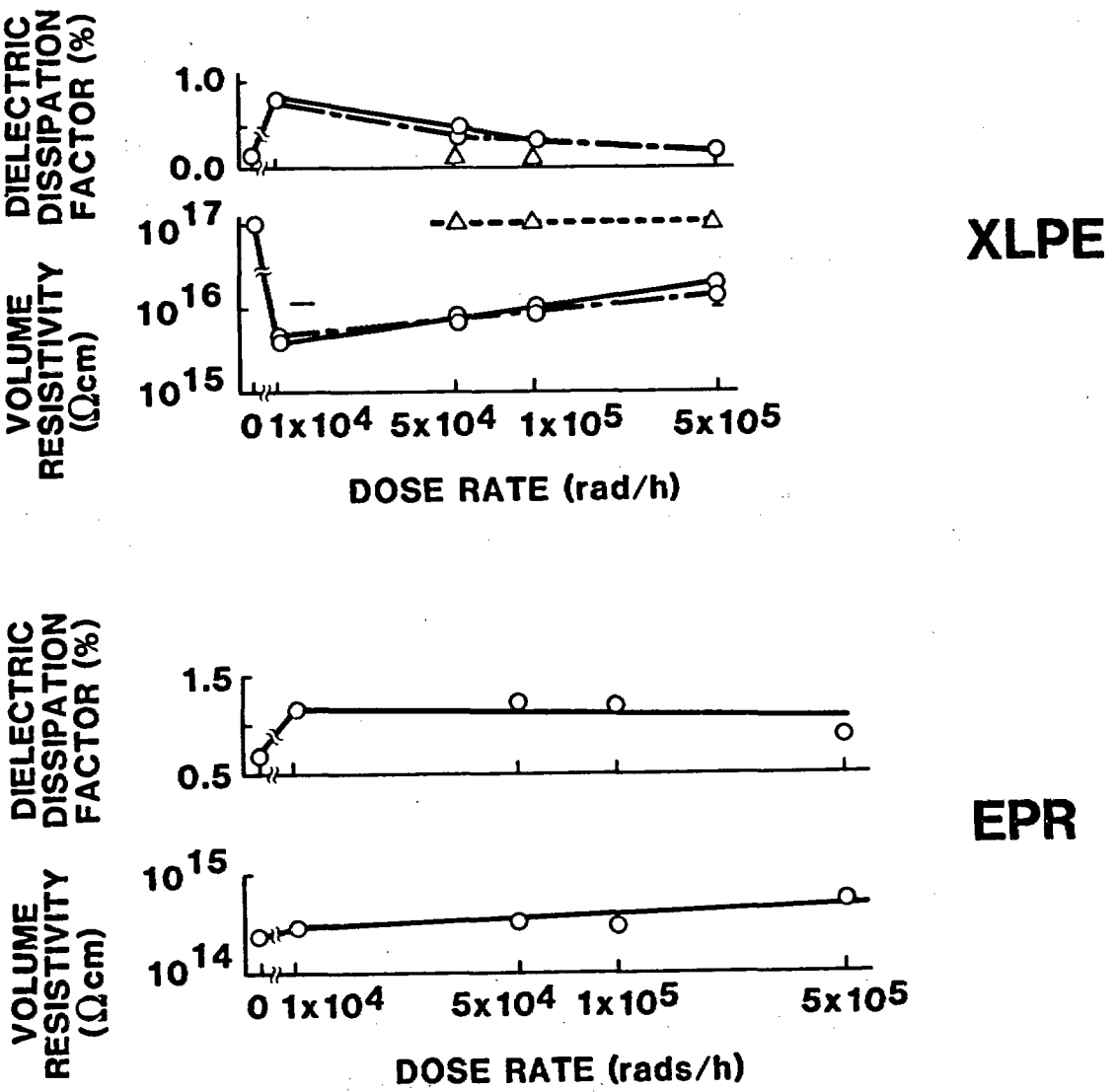

Figure 3. Dissipation Factor and Volume Resistivity vs Dose Rate (After Kuriyama, Ref. 16); Dashed Curve is for Oxygen-Free Atmosphere

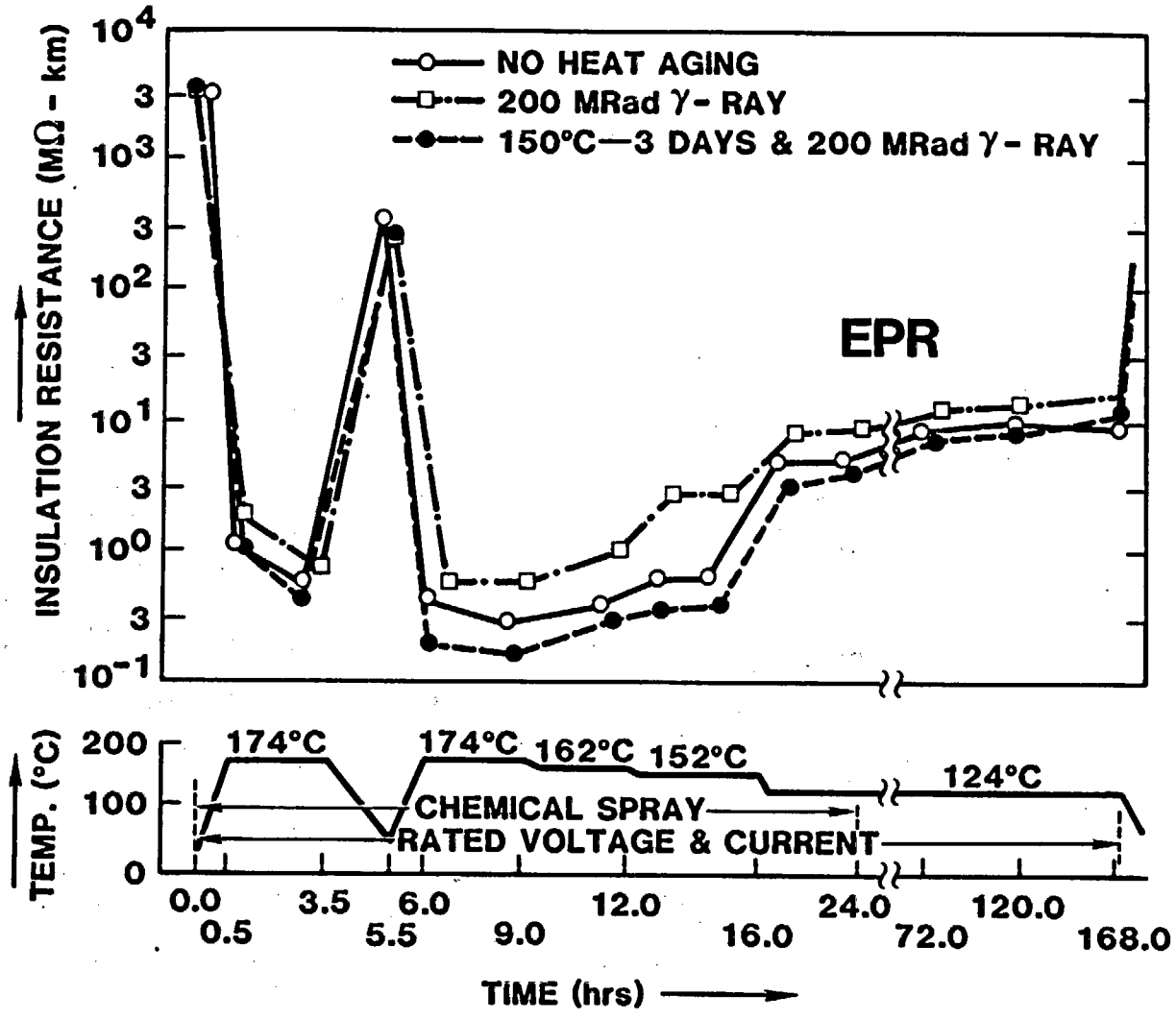

Figure 4. Insulation Resistance in Steam and Chemical Spray Environment (Flame Retardant EPR) (After Murata, Ref. 18)

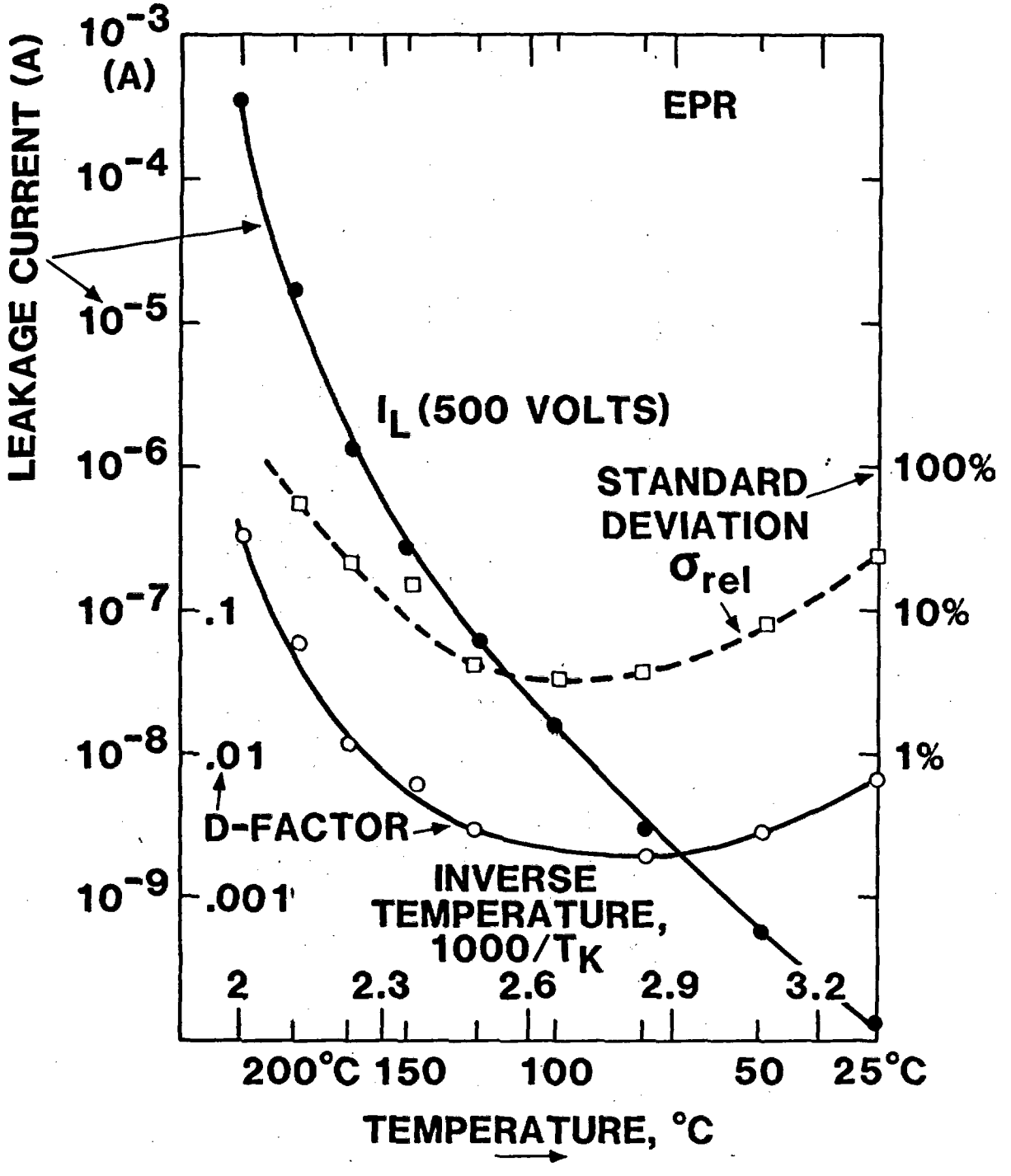

Figure 5. DC-Leakage Current I_L for 1-m Cable Length (Standard Deviation of I_L is σ_{rel} and Dissipation Fac-Factor is D)

is current dependent, the second depends on the applied voltage. The cable presently under investigation, AWG #14, has a conductor resistance of 0.00828 ohms/m at room temperature. At 100°C, this value is increased by a factor of 1.43. At the maximum rating, 20 A, the cable current causes heat generation of 4.74 W/m at 100°C, and somewhat more at higher temperatures. The installation has to be able to carry this heat flux away, and usually is amply dimensioned to do this. Therefore, dielectric losses may add a comparable amount of heat generation without undue consequences. To be conservative, we will stipulate that dielectric heat input will not exceed 20% of the permitted current heat generation. Dielectric losses are therefore limited to 0.95 W/m for the present cable.

For dc, the dielectric losses are U^2/R where U is the applied voltage and R is the leakage resistance of the cable per unit length. For an applied voltage of 480 V, it is found that R must be larger than 0.24 Mohm•m to keep the losses under 0.95 W/m. The cable average measurement in Figure 5 (with an applied voltage of 500 V and a leakage current of 0.4 mA at an equilibrium temperature of 225°C) yields an average value of 1.2 Mohm•m at the highest experimental temperature. This cable design can thus be assumed to be safe from thermal runaway up to 225°C.

For ac, the losses are essentially electronic and therefore generally less than for dc, which contain an additional ionic conductivity. For a D-factor of 0.35, the ac losses, $U^2\omega CD$, with C being the cable capacitance per unit length, are about 0.015 W/m for the example in Figure 5 and are therefore negligible.

The above deductions assume that the loss resistance and the D-factor are reasonably uniformly distributed along the cable, i.e., that there is no "bad spot" solely responsible for the leakage current. For the measurements in Figure 5, this is assured by the standard distribution value for the 10 leakage current measurements, which reaches only a factor of 2 for the highest temperatures. Unfortunately, many measurements in literature are made only with one or a very few cable samples.

Not many measurements in literature are made at temperatures as high as 225°C. If we wish to determine from such lower temperature measurements (e.g., Figure 4), the highest safe operational temperature, we may (for EPR) use the leakage current curve in Figure 5 for scaling. It is found, that a cable exhibiting 96 Mohm•m at 175°C would show 7.5 Mohm•m at 200°C and 0.24 Mohm•m, the critical value, at 225°C. The cables used for obtaining Figure 4 would therefore still be usable up to 225°C.

The two examples above may have involved cables of above average quality. At Sandia, for some EPR power and control cables, lower values of R have been measured than for these examples. A conservative value for a safe temperature is 190°C. Permitting a minimum resistance of 0.24 Mohm•m at 190°C, scaling as described leads to a minimum resistance of 1.3 Mohm•m at 175°C. Values in the neighborhood (but below) this figure have so far been only observed on control cables of one manufacturer. As control and signal cables work at much lower voltages than the above discussed power cables, thermal runaway is not a problem for the former. Nevertheless, addition of a leakage vs temperature test to qualification procedures may be helpful for selection of the best cables.

Temperature increases up to 190°C (and probably 10° higher) do not lead to dielectric failure in EPR power and signal cables. For an XLPE configuration, the conductivity is an order of magnitude lower than for EPR and the temperature dependence is about the same (Ref. 15, Figure 4-2). The failure probability for this XLPE cable is therefore lower. Generally, it may be assumed (considering the wide range of resistivities for EPR discussed above) that XLPE properties are of comparable magnitude.

3. Comment on Circuit Failure

The present work deals only with primary cable failure, i.e., complete breakdown of the cable proper. The above discussion of leakage contains data, however, which permit useful comments on circuit failures.

The first phenomenon of concern is circuit starvation - loss of so much current through leakage, that the load does not receive enough power. A 100 m long circuit is considered. At 480 V, 190°C, and the permitted 0.24 Mohm•m resistance, the circuit would lose 200 mA, which for a power circuit is unimportant. (At 175°C, a circuit using the cable of Figure 5 would only lose 0.6 mA.) For a signal cable operating at 50 V, the losses would be a tenth of the above values or less. A 10% current loss would cause unacceptable misreadings, if the information readout is current dependent.

Similarly important is crosstalk, particularly between power circuits and control circuits. As stated above, a power circuit with a marginal cable may generate a stray current. However, installation regulations demand total spatial separation of power and signal circuits; where this is the case, no problem exists. Signal-to-signal circuit crosstalk is mitigated by lower voltages. Instead of the 200 mA of stray current in the above example, 20 mA would be available. If a small part of this (e.g., 2 mA) enters a signal line, the accuracy of indication would suffer.

4. Other Phenomena

While radiation is applied, the conductivity of insulating materials is enhanced due to additional carrier generation. This phenomenon should be independent of temperature but could conceivably cause excessively high currents during accidents. Figure 6, taken from a paper by Murata et al.,[18] shows measurements on EPR cables aged in a variety of ways. Resistivity varies by less than a factor of 2, and is not proportional to the dose rate. Extrapolating to a dose rate of 10 Mrad/h, dose rates comparable to those expected in an accident, indicates that a parallel resistance of more than 100 MΩ would appear across a 1-km length of cabling. At higher temperatures, the effect would be overwhelmed by thermal-carrier generation.

The influence of humidity on cable resistivity is observable but small. Measurements by St. Onge et al. (Ref. 15, Figures 4-3 and 4-5) show an order of magnitude increase in conductivity for XLPE under extreme humidity (soaked cables) compared to dry conditions. A somewhat smaller increase is shown for EPR. The measurements quoted above (e.g., Figures 4 and 5) include the influence of humidity.

Cables immersed in water, as might be the case after an accident, may exhibit a particular form of field breakdown caused by water penetrating the cable along micro-fracture structures. A phenomenon named "treeing"[19,20] develops when tree-like fractures filled with liquid slowly extend into the insulators. This phenomenon is of importance at high field strengths. Data are not available for low operational fields, those smaller than 1 kV/mm for power cables. Treeing becomes less pronounced at high temperatures, while the influence of radiation is unknown. An experiment representing the probable worst case has been in operation for 16 months in our facilities. In this experiment, ten 1-m-long cables have been soaking in water at room temperature under field strengths 5-times higher than the operational level. No breakdowns have been recorded.

For a cable with very high insulation resistance, another breakdown effect has been reported in the literature.[20] A space-charge region may build up under irradiation, causing high local fields and a discharge breakdown. In reactor circuits, the effect would be strongly mitigated by low circuit impedance; it can be disregarded at higher temperatures, where higher conductivity would cause the space charge to leak off.

5. Summary

The above discussion has been brief. A more comprehensive study of basic electrical breakdown mechanisms and of literature data has been performed and many more preliminary tests have been evaluated.[21] We believe it has been adequately

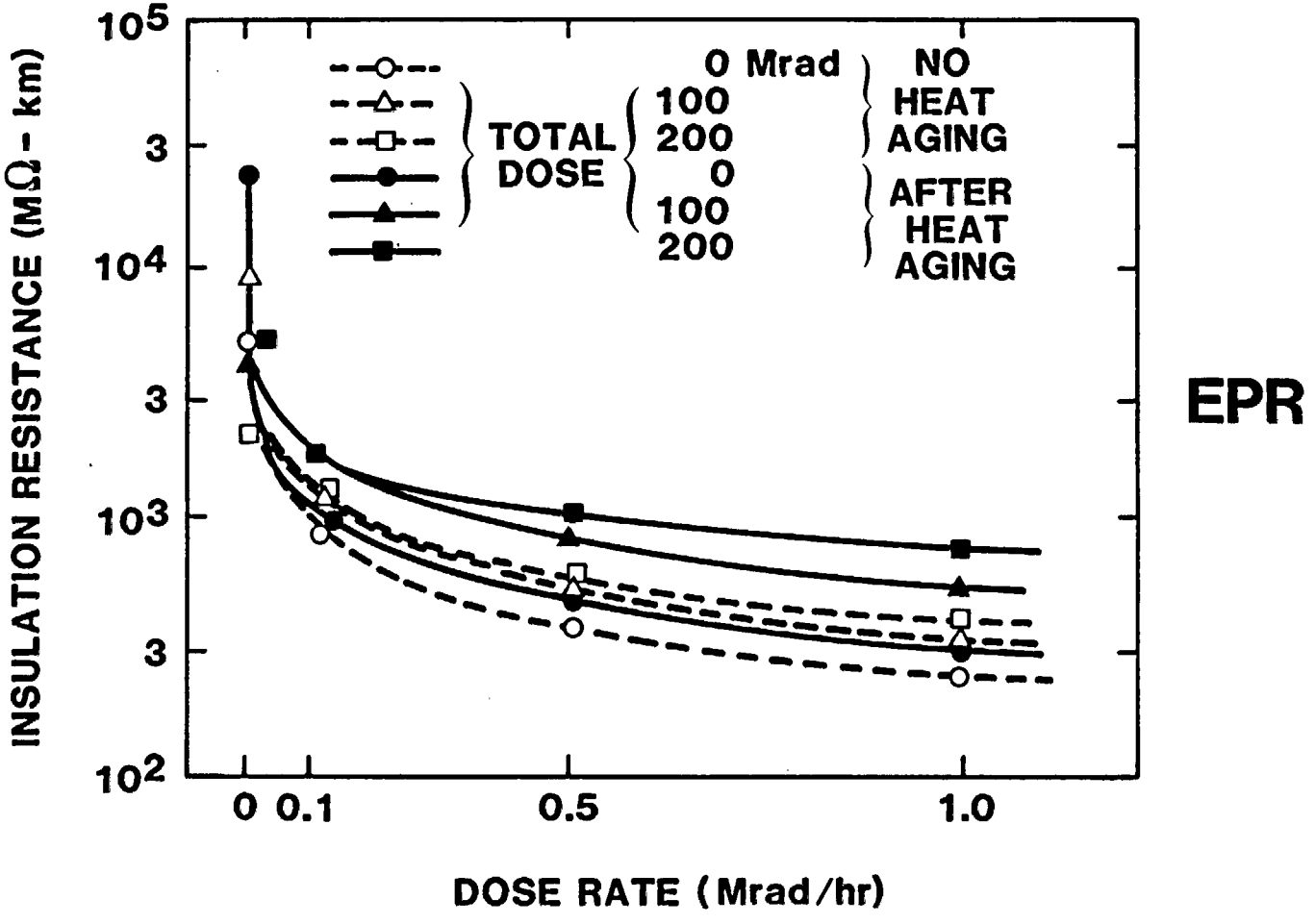

Figure 6. Effect of Dose Rate on Insulation Resistance (After Murata et al., Ref. 18)

shown that a purely electrical failure is highly unlikely up to temperatures of 190°C. The discussion now turns to electromechanical phenomena.

III. TEST INSTRUMENTATION

1. Dedicated Test Facility

To permit long-time aging and creep measurements, a dedicated facility for the present experiments has been established. Figure 7 shows an overview, which includes seven temperature-controlled heat chambers, equipped with circulation fans and, on the left, additional calibrated digital thermometers. A common 480 V ac power supply, under the third chamber but not clearly visible in Figure 7, permits application of an electrical stress field to any cable; breakdown of this field is detected by short-circuit indicators. In each of the heat chambers, six sections of cable are hung, under mechanical tension, over 4.8-mm diameter cylindrical supports. An additional 40 unstressed samples were put into each chamber at the beginning of the tests.

The center of the test area is occupied by three 10-m-long iron pipes, each 50-mm in diameter and surrounded by 25-mm-thick insulation (Figure 7). In each of the pipes, six long cables are heated by passing from 20 to 30 amperes of dc current through the cable conductors. Thermocouples are positioned at 1.7-m intervals on the inside of each pipe; the common dc power supply, and some of the surveillance instruments, are seen in the foreground of Figure 7. The heating circuit, with adjustment resistors that keep the temperatures in the pipes at 95°, 135°, and 165°C, respectively, is shown in Figure 8.

A rail, on which an instrument cart can be moved precisely to any point on the heat chambers, is visible on the right side of Figure 7. A theodolite and an X-ray camera are mounted onto this cart (Figure 9). These instruments are used to precisely align the cable tensioners inside the heat chambers and, at regular intervals, to X-ray the cables to detect deterioration. To simplify this, precise stop points are marked on the rails, enabling the position of the optical center of the theodolite or X-ray camera to be accurately located.

2. Cable Tensioners

A cable-tensioning device, which is designed to permit precise creep measurements, is mounted in each of the heat chambers (Figure 10). Six cable samples are positioned over gooseneck-shaped supports and stretched by lead weights (visible at the rear of the mounting struts in Figure 10). For three of the six cables, the maximum operational electric field is maintained between cable wire and support by applying the highest operational ac voltage, 480 V. The three short-indicating circuits are seen located on the right in Figure 10.

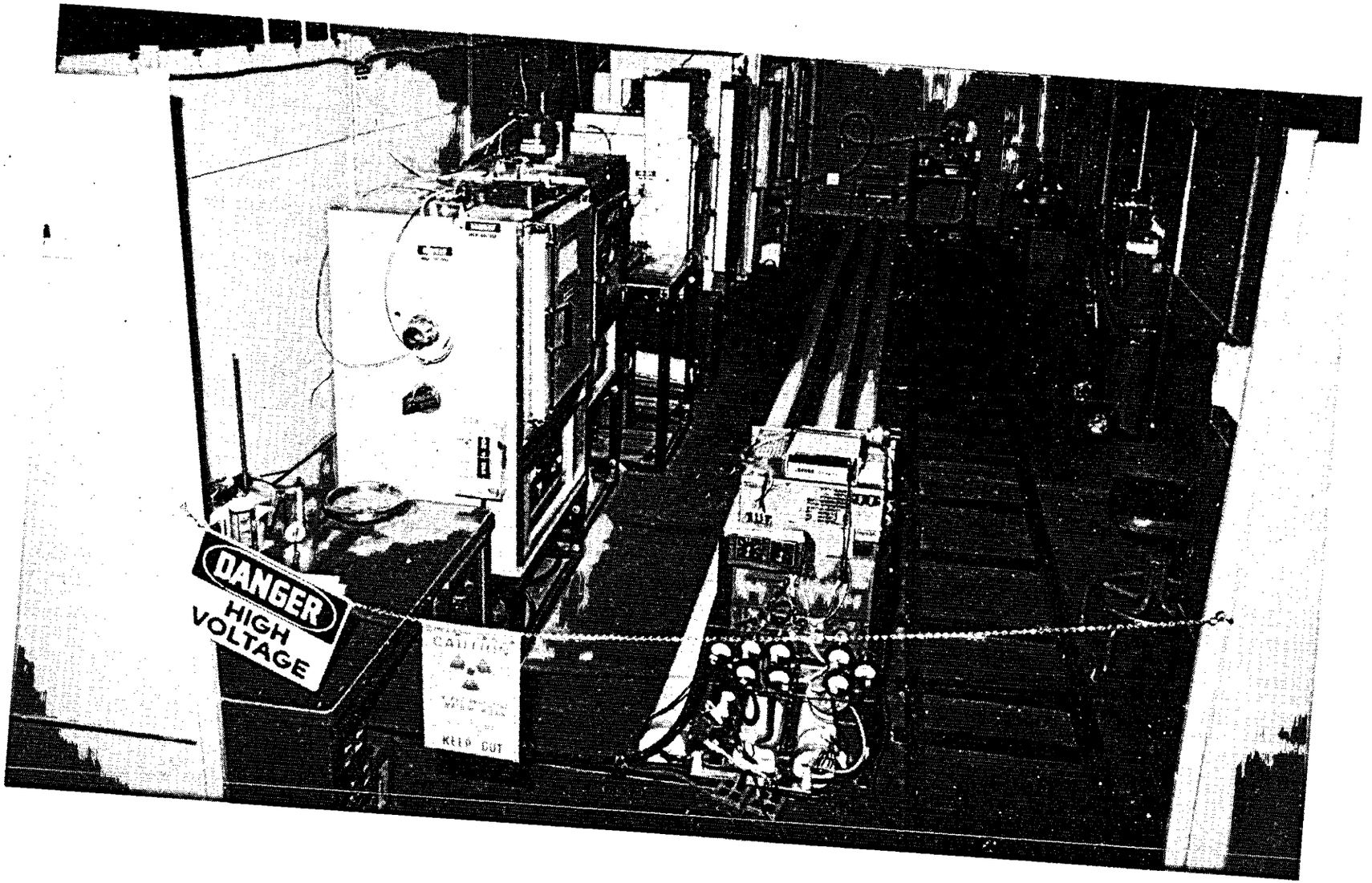

Figure 7. Overview of Dedicated Test Facility

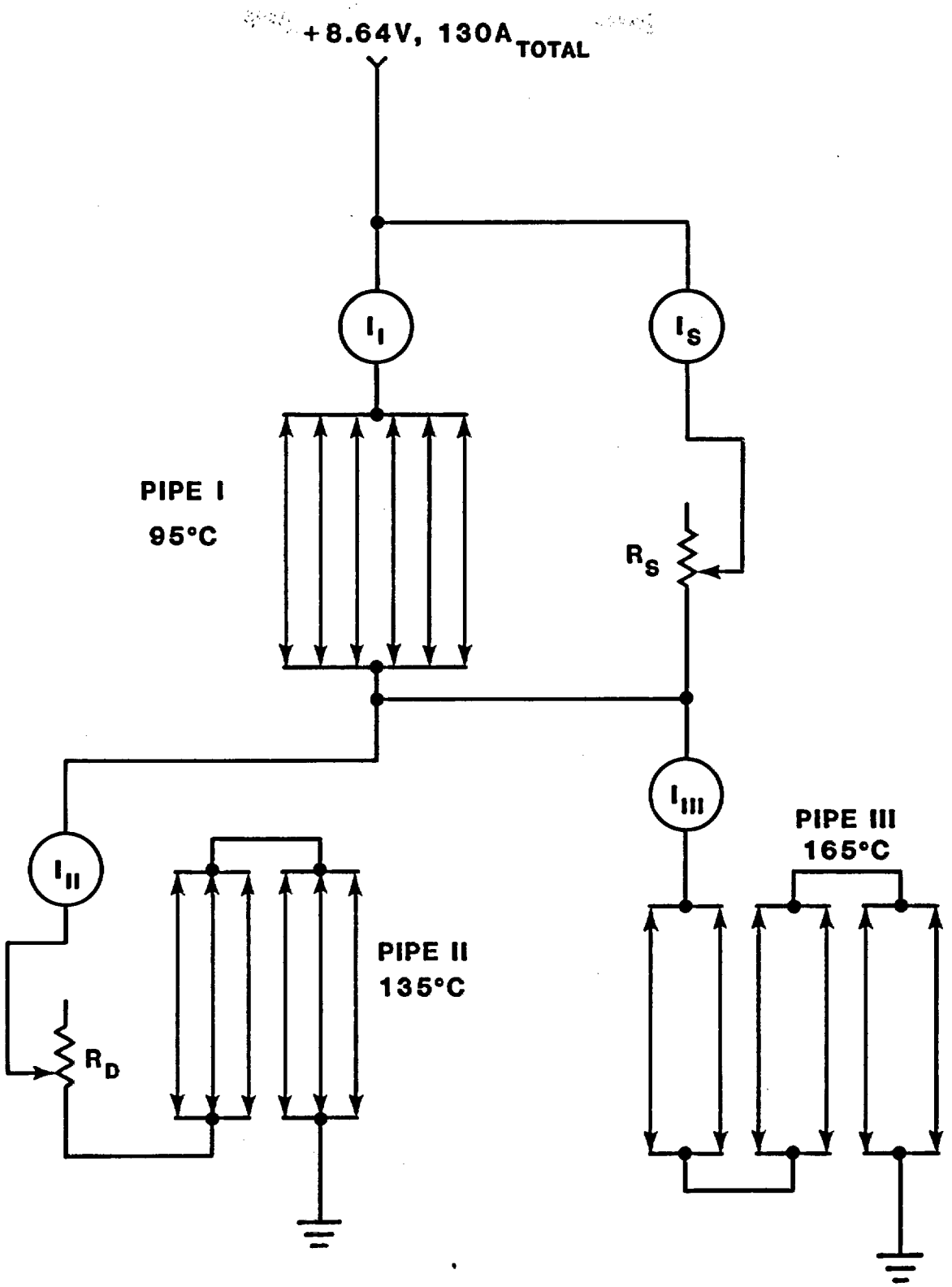

Figure 8. Schematic of the Heating Circuits

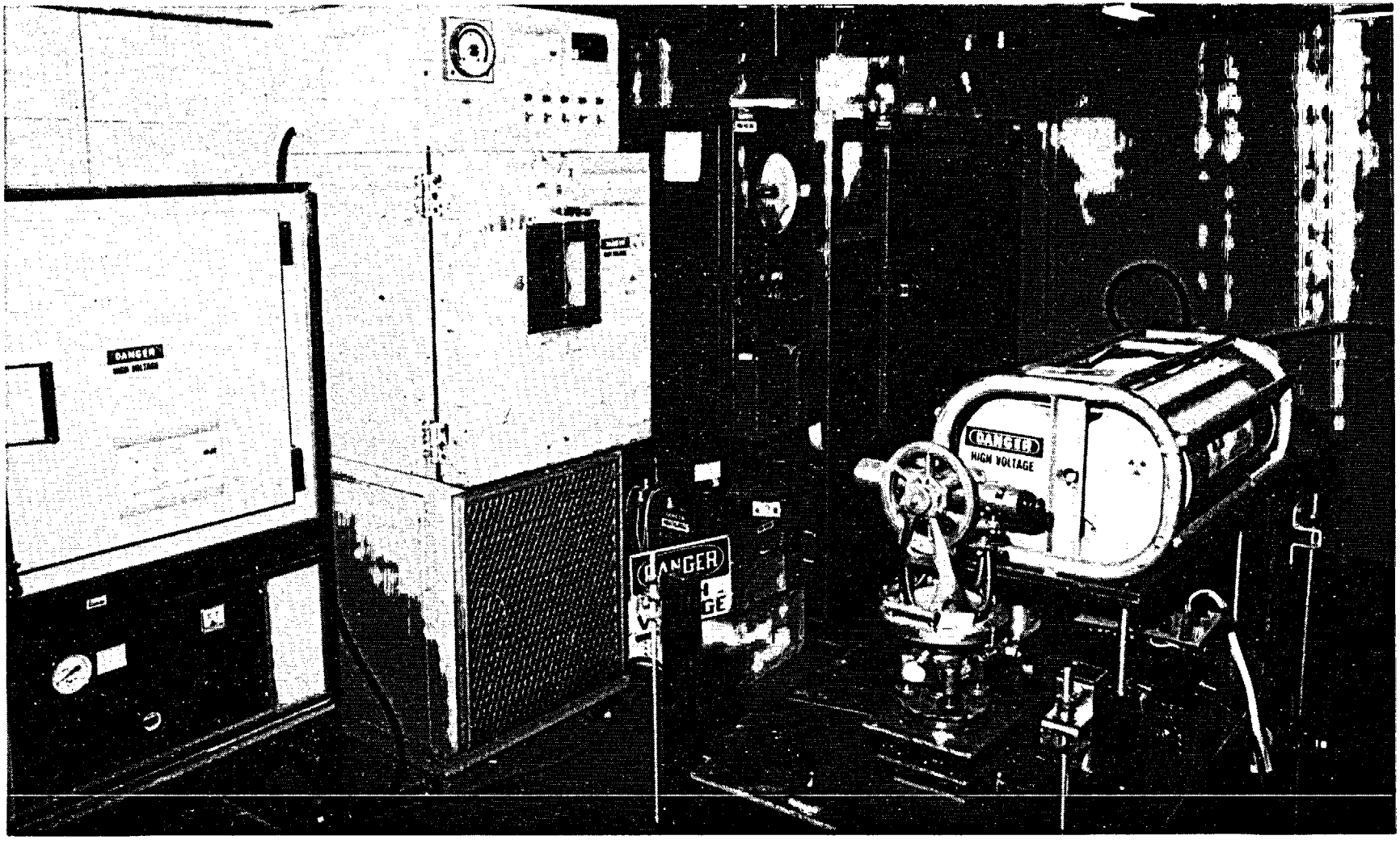

Figure 9. Photograph of the Instrument Cart

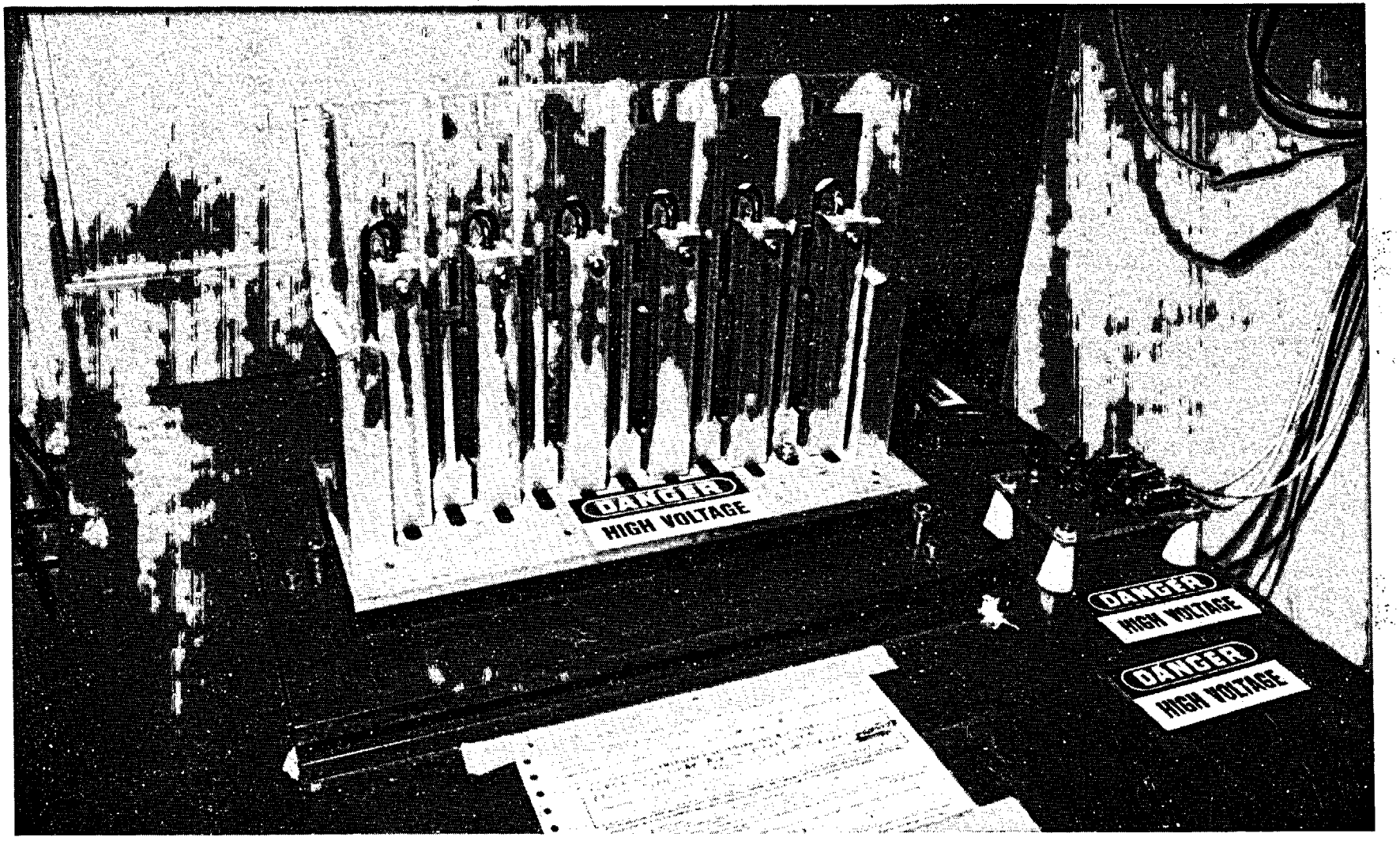

Figure 10. Photograph of the Tensioner

In the center of the horizontal part of each gooseneck structure (Figure 11), a 1-mm-diameter precision-drilled alignment hole is provided. By means of setscrews, the six holes of each tensioning device are pointed to the optical center of first the theodolite and later, automatically, of the X-ray source. A curved film cassette can be attached to the support frame shown in Figure 10, with the film position indicated on the right in Figure 11. One X-ray picture will furnish a shadowgraph of the six cables on each tensioner; of interest are the areas showing the gooseneck projection with holes and the cable wires. An important quantity to be measured is the distance, y, between goosenecks and cable wires (Figure 11). This "remaining creep distance" is extensively discussed below. To avoid the introduction of sporadic density gradients on the pictures, X-ray exposure, film development, and copy enlargement (a factor of 30) must be done very carefully. A mechanized installation in Sandia's Nondestructive Testing Department provides this service.

The calibration hole in the horizontal part of the gooseneck support has a second purpose. It is needed not only for original alignment, but also furnishes a correction if, as is unavoidable, the support distorts during many months of stress, sometimes at high temperatures. Originally, the illumination source is located on or close to the axis of the cylindrical hole, as indicated in Figure 11. In this case, the picture of the hole will be a circle, and the projection of the creep distance, y, will be correct within a few microns. As the gooseneck bends down or up, the illumination source will appear to move in the opposite direction, and the rear or front end of the gooseneck will shadow off part of the creep distance, y. The image of the hole boundary then becomes nearly elliptical with a horizontal major axis. A sideways motion of the support causes a tilt of the ellipse's major axis by some angle ϕ. From the ratio of the ellipse's measured axes, and the measured angle ϕ, a correction for the real or apparent decrease in creep distance, y, is found.

The analysis of the correction[22] is straightforward although lengthy. Up to now, the corrections obtained were generally less than 20 μm. For the present dimensions of the gooseneck support diameter (4.76 mm), the alignment hole diameter (1 mm), and the distance to the light source (2 m), the correction for vertical distortion (angle $\phi = 90°$) is shown in Figure 12. For angles ϕ less than 90°, the correction quantity is determined by multiplication with $\sin \phi$; pure horizontal motion of the gooseneck does not require a correction for y. In Figure 12, the expected "uncertainty" in the image as seen in the X-ray pictures is also indicated. This uncertainty is due to the finite size of the present source (2 mm).

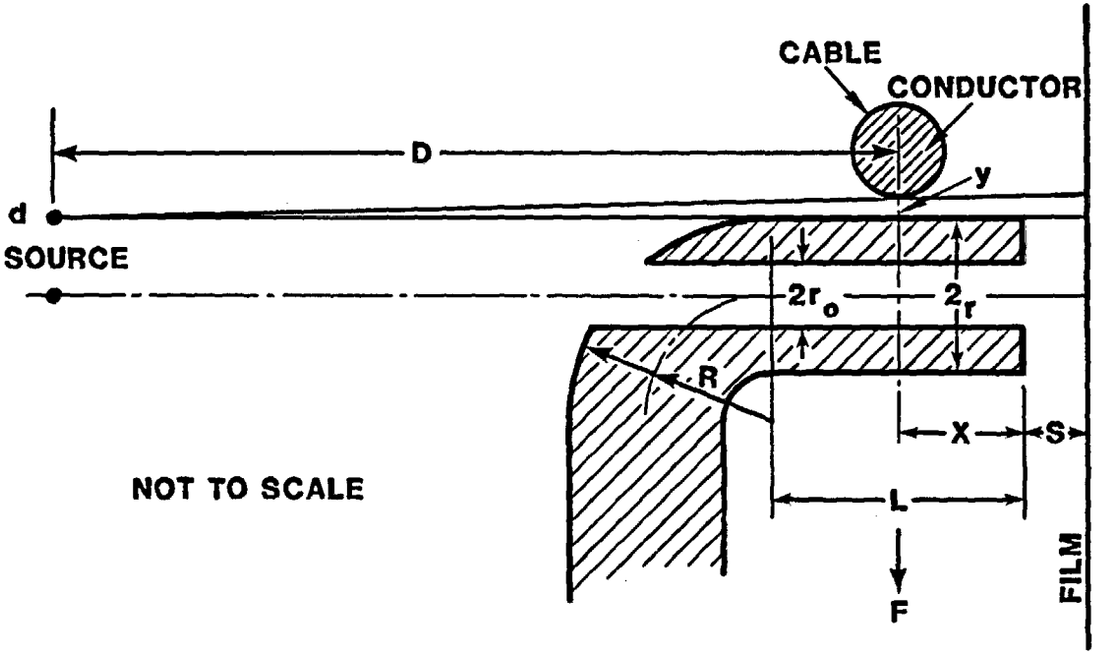

Figure 11. Cross Section of Gooseneck Support and Cable

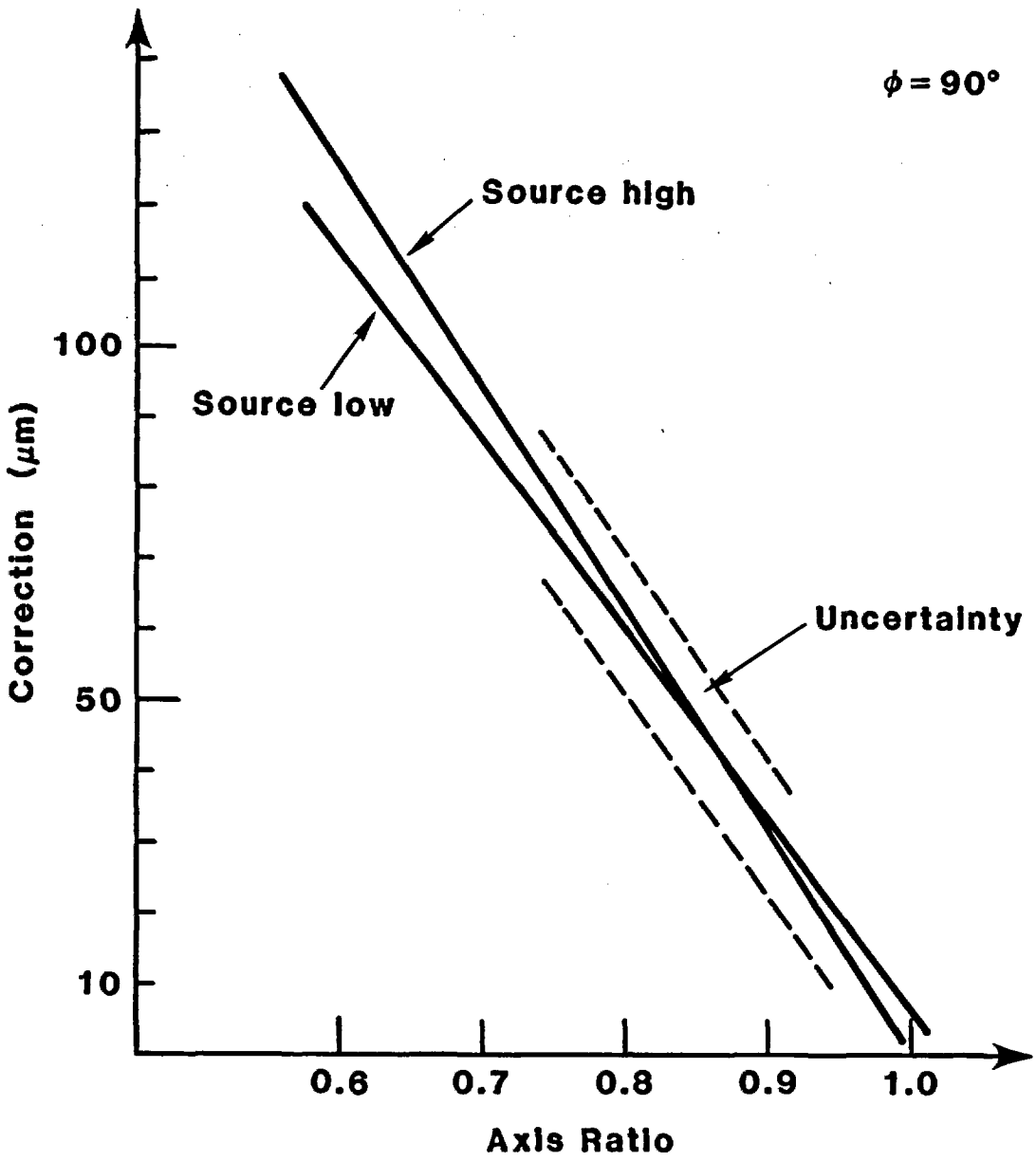

Figure 12. Correction for Creep Distance as Function of the Ratio Between Ellipse Axes (for cases where angle ϕ = 90°)

3. Special Apparatus

For cracking experiments, cables have to be bent reproducibly. Figure 13 shows a simple jig developed for this purpose. A movable lever, connected to a vertical post, wraps the cable around a cylinder 12-mm in diameter. It usually took about 10 seconds to bend the cable into a hairpin structure; uniformity of motion was attempted.

Located outside the test facility (Figure 7) is a setup to test the "treeing" mentioned in Section II. Cables are placed in a container partially filled with a saline solution and connected to a power supply (Figure 14).

For meaningful loss measurements at operational voltages, a special high-voltage impedance bridge has been developed. Additionally, materials-shrinkage experiments were aided by a simple overflow-volume measuring device, which used a fluid consisting of an alcohol-water mixture to reproducibly wet the cable samples investigated.

In summary, a considerable number of devices for holding, bending, stretching, and cutting cables reproducibly were developed and tested, particularly during the preliminary experimentation phase of this investigation. Several of these devices are described in greater detail in Reference 22.

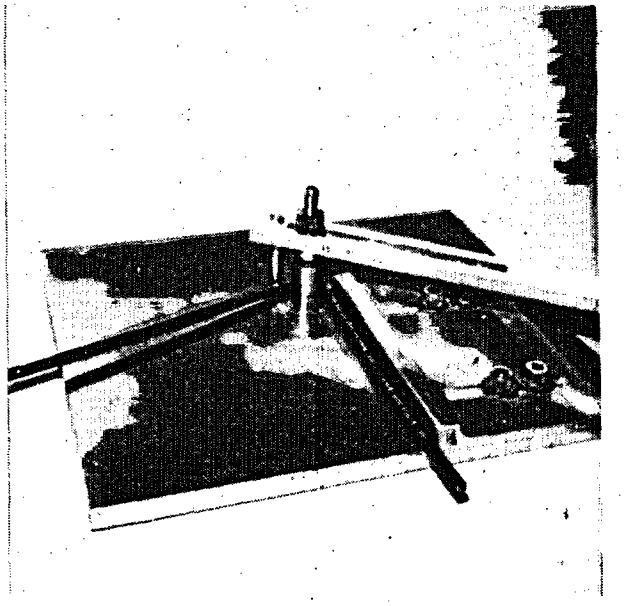

Figure 13. Cable Bending Tool

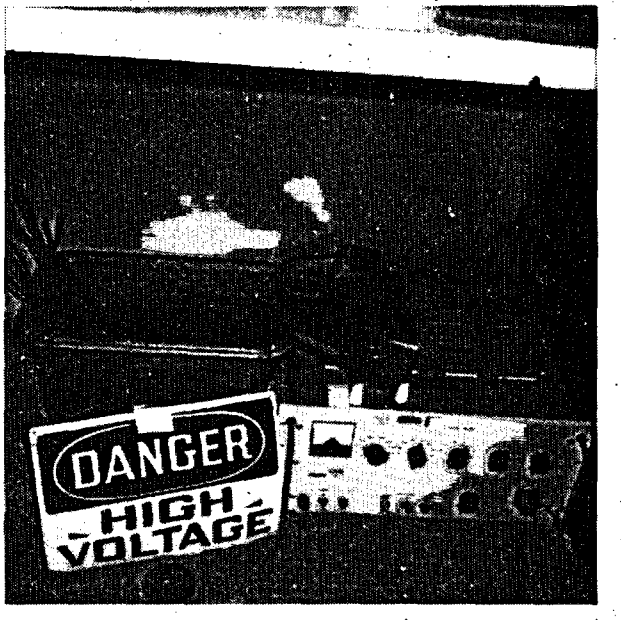

Figure 14. Setup for the Treeing Test

IV. CREEP SHORTOUT

1. General Comments

A cable is stretched by an applied force, F, over a surface with a radius of curvature, r. At elevated temperatures, the metal wires will creep through the softened polymeric insulation and cable jacket; after some time, metallic contact between cable wires or between the wires and the cable support may occur. The present discussion is limited to the simplest case where the cable consists of a single wire surrounded by an EPR insulator and a Hypalon jacket.

The situation of concern involves large compressive strains with values approaching unity. There is, however, nothing in the literature concerning such large strains. As a result, an essentially experimental investigation backed by computer modeling was undertaken. To introduce basic concepts, an attempt will be made to first draw conclusions from existing pertinent data for small-strain situations.

The low-strain behavior of polymeric materials including rubber has been thoroughly investigated.[24] Even the long-term or "aging" phenomena of these materials are subjects treated in textbooks.[25] Unfortunately, most published work is limited to temperatures below transition temperatures, which means that only the lower regions of the temperature range of present interest are covered. (For EPR the transition temperature is not well defined, and the transition is not severe since only a small percentage of the polyethylene incorporated into the compound shows a crystalline melting point; the "transition" lies between temperatures of 70° and 90°C.[26])

At low temperatures and low strain rates, creep is a linear function of applied stress, σ, and a function of a time dependent "creep compliance," J(t), or its inverse, the creep modulus, M(t). The creep strain, ϵ, is given by

$$\epsilon = \sigma \cdot J(t) = \sigma/M(t) \qquad (1)$$

where σ is assumed constant, and J or M is measured at a constant temperature, T.

For the same material, curves representing the time dependence of J, measured at different temperatures, starting times, and stresses, are similar. Consequently, the curves can be obtained from one another by translation of the horizontal or vertical or both axes, and by scale changes. Figure 15 shows a Bell Telephone Laboratories "master curve" obtained by shifting many measurements to obtain overlay with a room-temperature curve.[27] At room temperature and within the validity range, Figure 15 predicts a strain of less than 4% in 40 years for high-density polyethylene (HDPE) under a

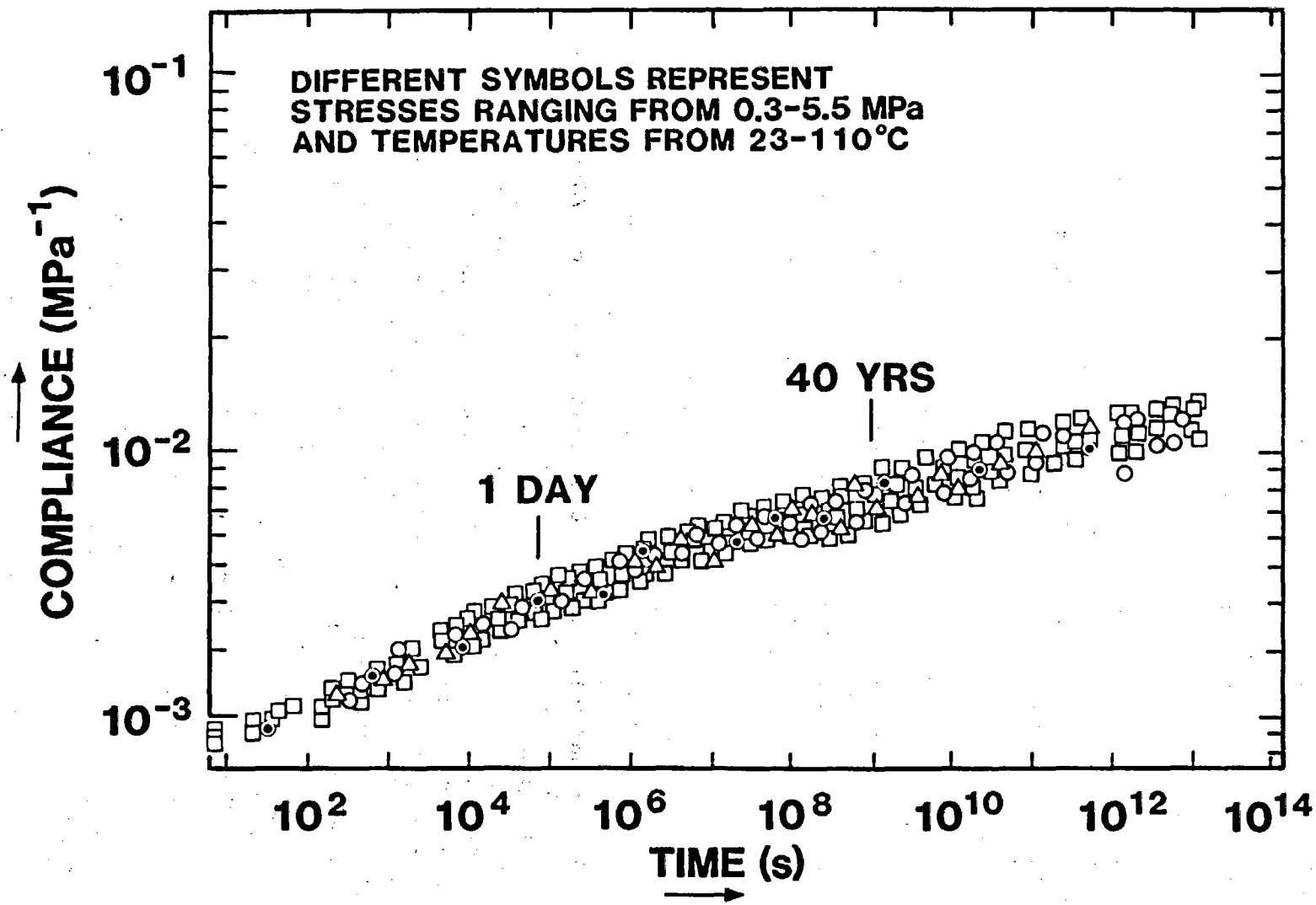

Figure 15. Room-Temperature Master Curve for High-Density Polyethylene in Creep (After Aloisio and Brockway, Ref. 27)

stress of 600 psi (4.1 MPa). This confirms that creep is exceedingly slow under most circumstances.

Instead of Equation 1, another method may be used to determine creep strain.[18] An "effective viscosity" is defined as

$$\eta = dt/dJ \qquad (2)$$

when the plastic is considered a fluid, and Stokes' equations are used to determine the movement of the boundaries to which the stress is applied. The η values obtained from Equation 2 are usually very high. For the example, the effective viscosities vary from 10^9 Pa•s at the left side to 10^{19} Pa•s on the right side of Figure 15.

Attempts have been made to extend Equation 1 to strains of several percent (Ref. 25, p. 157). Linear extrapolation appears to be justified in a number of cases, but experimental proof has yet to confirm this. The model using Equation 2, however, appears to be more suitable for high-strain problems. It is significant, however, that these models are useful only up to a critical stress,[27] which has to be determined experimentally.

Higher temperature creep data have been measured by St. Onge[15] for crosslinked polyethylene and EPR; the detailed composition of the materials, however, is proprietary. Figure 16 is the creep modulus, M, plotted versus time for a number of compositions, with the material kept at a temperature of 70°C. The creep modulus versus temperature, after a 10-hour exposure, is shown in Figure 17. The data pertain to compressive creep, of interest here, and permit, with some extrapolation, a crude order of magnitude estimate of the creep effects expected. At 70°C, a representative containment temperature, an EPR sample may have a creep modulus of 2.8 MPa after 10 hours (the worst case in Figure 17). As will be discussed below, stresses of 2.8 MPa are quite reasonable if a 1-mm diameter wire is pulled by a 0.5-kg weight over a surface whose radius of curvature is a few millimeters. The resulting strain would be unity, i.e., the conductor would have cut through the insulation and jacket. This conclusion is out of the validity range of small-strain theory, but raises concern.

2. Preliminary High-Strain Experiments

A number of experiments were performed to obtain data on high-strain behavior and at the same time to demonstrate actual creep shortout.[22] The experiments will be summarized here.

a) Shortout Observation -- Cable samples were strung over a supporting cylindrical bar, stretched by weights, and exposed to various temperatures. Figure 18 shows the relative

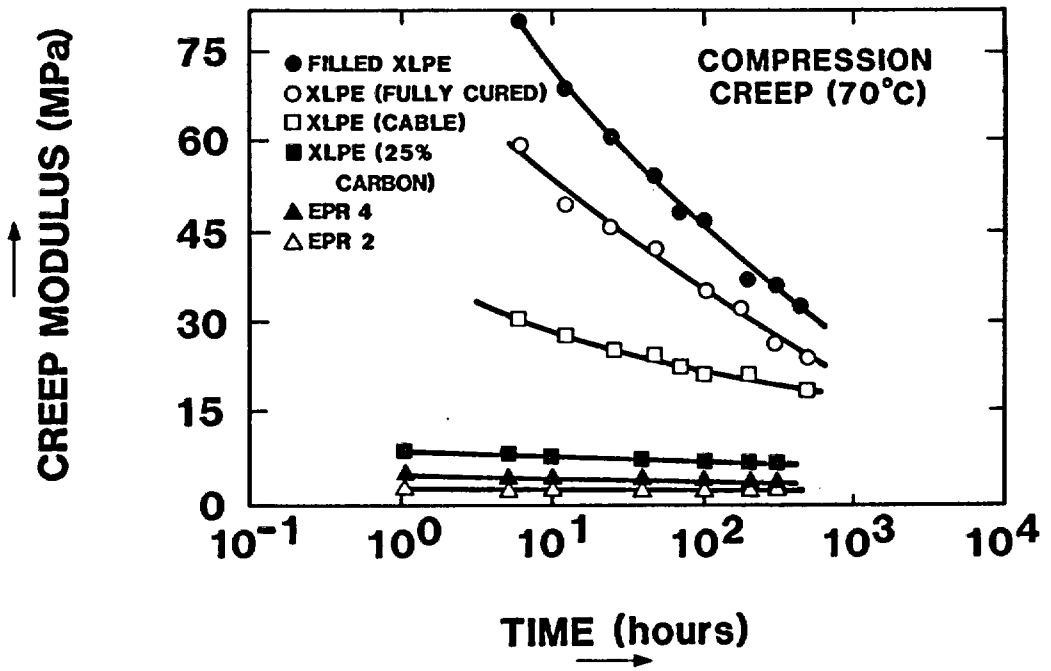

Figure 16. Compression Creep Modulus for EPR and XLPE at 70°C as a Function of Time (After St. Onge, Ref. 15)

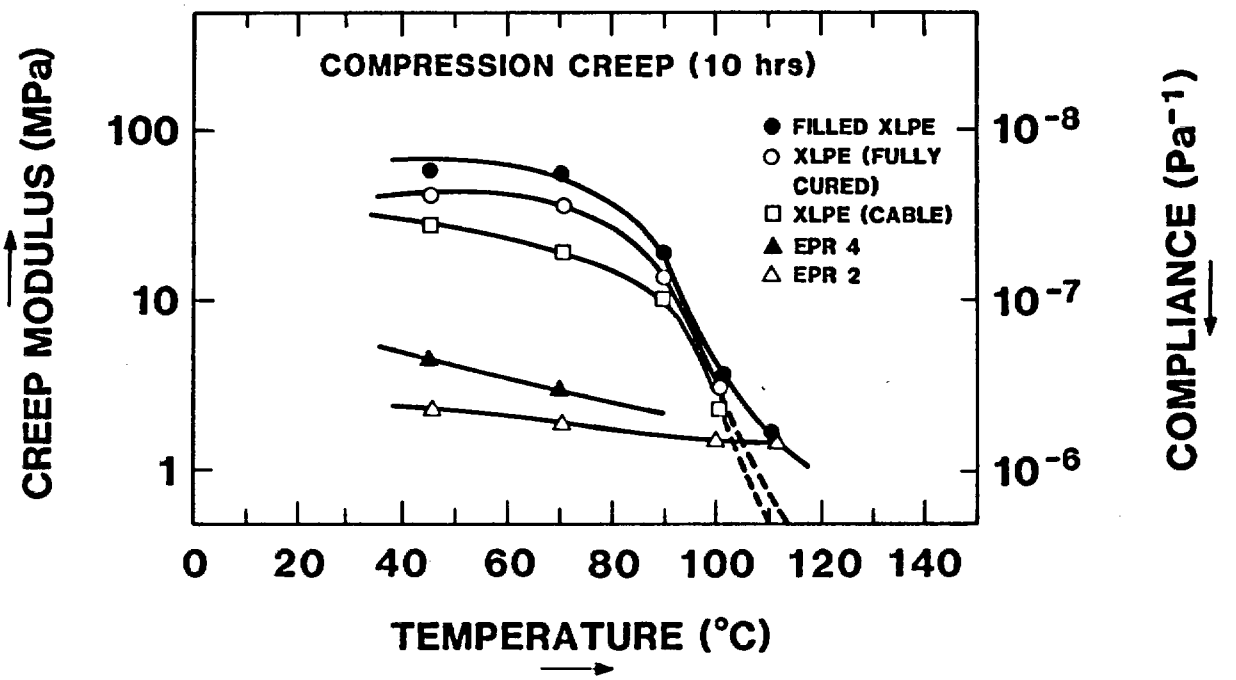

Figure 17. Compression Creep Modulus for EPR and XLPE at 10 Hours as a Function of Temperature (After St. Onge, Ref. 15)

sizes and shapes of cable and supports. A second supporting geometry (sharp corner) is shown in Figure 19. For determination of stress from some known stretching weight, an effective support area must be estimated. For the geometries in Figure 18, the effective area, A, should be proportional to the wire radius, r_w, and the curvature radius of the support, r_s, such that

$$A = kr_w r_s \qquad (3)$$

where k is the proportionality constant.

For the corner geometry of Figure 19, the support radius r_s is replaced by the cable radius, r_c. The proportionality constant, k, should be of the order of unity for both cases.

A detailed but preliminary estimate of stress distribution and support stress for the above geometries has been developed by Reaugh.[28] He finds that a square-root dependence of stress on applied force better fits observations than the generally used linear law. In Figure 20, Reaugh's solution of stress versus support radius are plotted for two stretching weights, 0.45 kg and 0.90 kg, and compared with the values from Equation 3, when k = 1. It is seen that a value of k = 0.3 would make the experimental approximation straddle Reaugh's solution. This latter value for k will be used in subsequent estimates.

For the preliminary tests, the stretching weights were unrealistically high, corresponding to 10-m to 30-m of cable overhang. The chosen support radii of curvature were lower than likely in an electrical installation. A considerable number of creep shortouts occurred; they are listed in Table 2.

All cables tested were of the standard design used throughout this investigation. The seven-strand copper conductor had an average radius of 1.15 mm, while the EPR insulation and the Hypalon jacket had thicknesses of 0.74 and 0.51 mm, respectively. In Table 2, the experimental arrangements are compared. Stresses estimated from Equation 3 with k = 0.3 are included, along with temperature history and the number of experiments for each exposure sequence. Electrical stress was not continuously applied. Creep shortouts were measured with a low voltage ohmmeter. In a number of cases, the jacket was still present at the end of the exposure, although somewhat reduced in thickness, while the insulator was totally squeezed out; these cases are identified in the last column. In the test listed on the bottom row of Table 2, the heat spike indicated was 300°C applied to the specimen for one hour before the test. The compilation in Table 2 demonstrates that at high temperatures (175°C) and high stresses (2 MPa or about 300 psi), shortouts occur readily and quickly. It is difficult to scale the measurements to lower stresses and longer

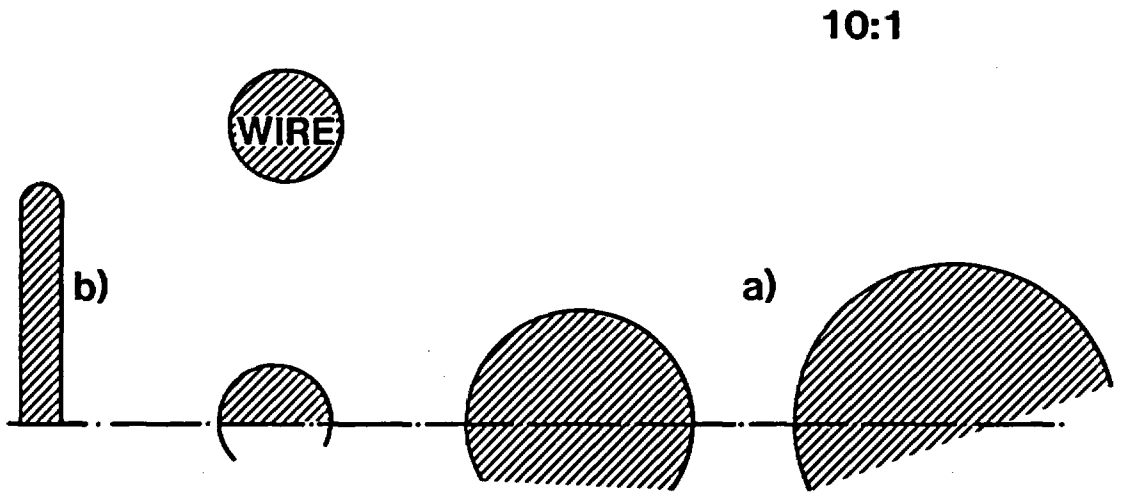

Figure 18. Relative Sizes and Shapes of Cable and Supports

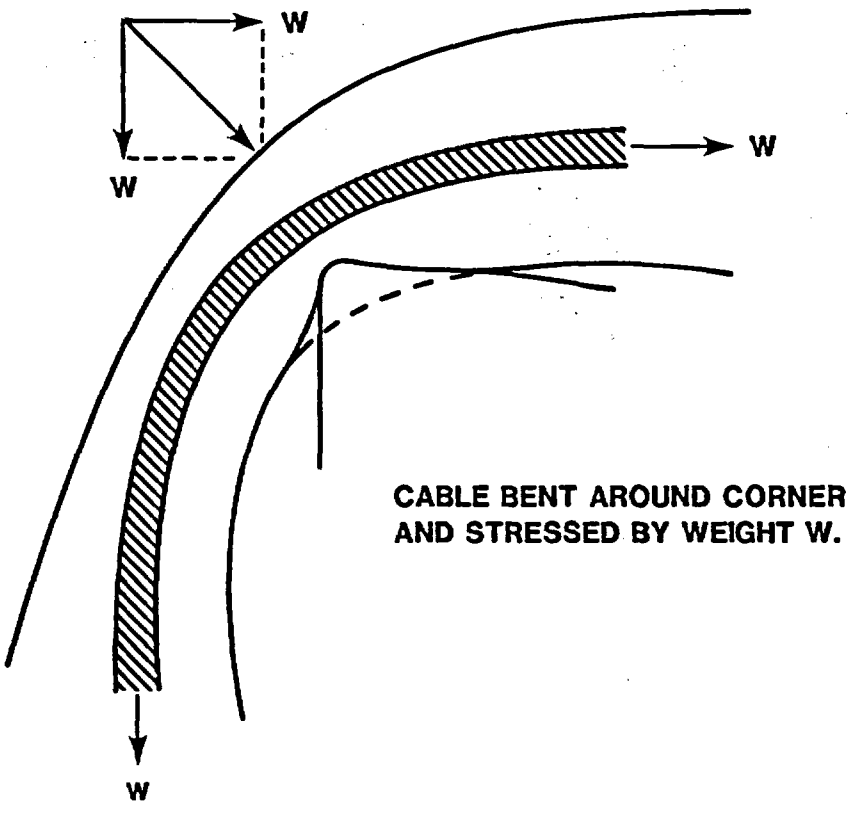

Figure 19. Corner Geometry and Force Distribution

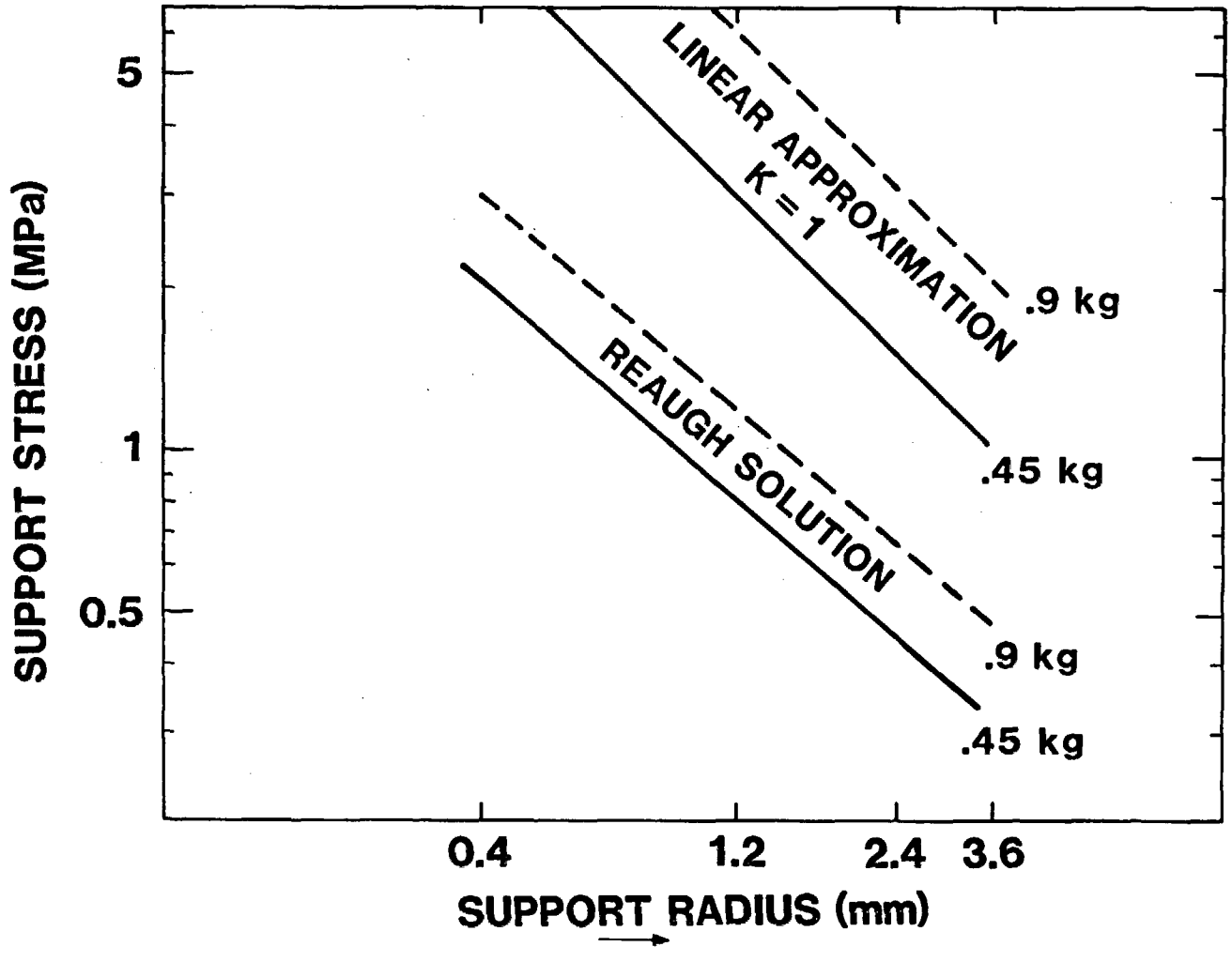

Figure 20. Stress on Support Surface vs Support Radius

Table 2

Creep Shortouts

	Experiments	Nominal Stress (MPa)*	Temperature Exposure	Exposure Time (days)	Number of Experiments	Number of Shorts	Number of Squeezeouts
(a)	r_s = 1.2 mm	2	190°C, Constant	2.2	2	2	
	r_s = 1.2 mm to 3.6 mm	0.3 to 1	190°-175°C, Constant	2.2	10	0	
(b)	r_s = .4 mm	5	175°C, Constant	21	2	0	2
	r_s = .4 mm	5	190°C, Constant	1	12	0	4
(c)	Corner Geometry	2	0-225°C, Rising	5	10	10	
		0.7	0-225°C, Rising	5	20	1	
		0.7	0-225°C, + heat spikes	3	10	2	

*No electric field
1 psi = 6900 Pa

times, taking into account the aging processes affecting the cable.

b) Deformation Measurements -- At the end of the exposure, the cable samples were carefully cross-sectioned along the plane of the most severe deformation. The remaining thicknesses of insulator and jacket were then measured; Figure 21 shows a cut through a new cable and through a sample exposed to temperatures of 125°C and nominal stresses of 2 MPa for 1 day. The cuts were made after cooling to room temperature. It is seen that deformation is nonuniform, asymmetric and, in this example, accompanied by unraveling of the wire strands. (It is believed that the cutting process itself did not contribute noticeably to these distortions.)

For this investigation, the minimum thicknesses of remaining insulator and jacket are of interest. Not surprisingly, considerable scatter was found in the measured values. A main contributor to the measurement variations is the relative position of the wire strands with respect to the support structure. This is demonstrated in Table 3. It is seen that the average thickness of the composite layer (insulator plus jacket) may vary by a factor of almost 3, depending on whether a single strand or two parallel strands lie opposite the support and take up the weight of the cable.

It is evident from Table 3 that the cable insulator yields much more easily than the jacket. Insulator squeezeouts are relatively common while squeezeout of the jacket is rare. This fact complicates the detailed investigation of cable systems.

An illustration of the time dependence of creep is presented in Figure 22. For two different temperatures (125°C and 190°C), the thickness of the two plastic layers is plotted versus exposure time, with the nominal stress as a parameter; each point represents an average for two experiments. In the beginning the thickness is reduced very rapidly, because the contact area between cable and support is at first very small and the stress is very high. As exposure time approaches one day, the contact area approximates the nominal value of Equation 3 and creep rate decreases. At 190°C, the bottom diagram in Figure 22, a shortout of the two cable samples has occurred after just over two days; the two cables were in the "unfavorable" position indicated in Table 3 (a).

c) Conclusions and Comments -- From the measurements, it becomes clear that simple small-strain linear theory does not hold for the present extremely large-strain phenomena. In Figure 23, composite creep compliance has been calculated as a function of nominal stress for a 24-h exposure. The compressive creep compliance decreases strongly with increasing stress in contrast to the behavior of tensional or torsional creep compliance. It is not clear at this time what the

(a)

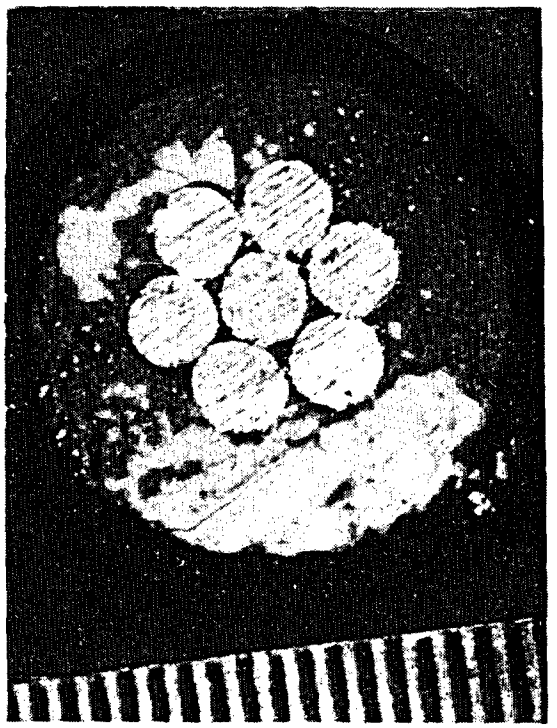

(b)

Figure 21. Cut Through a New Cable (a) and a Cable Stretched by 0.9 kg at 125°C for 1 Day (b)

Table 3

Position Dependence of Deformation

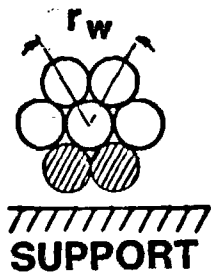

		Thickness (mm)			Strain		Composite
		Insulator	Jacket	Both	Insulator	Jacket	Strain
	Original Thickness	0.74	0.51	1.25	----	----	----
(a)	Remaining Thickness (mm)	0	0.07	0.07	1	0.86	0.94
		0	0.09	0.09	1	0.82	0.93
		0	0.10	0.10	1	0.80	0.92
	Avg:	0	0.0867	0.0867	1	0.83	0.93
(b)	Remaining Thickness (mm)	0.01	0.20	0.21	0.98	0.61	0.83
		0.05	0.21	0.26	0.93	0.98	0.79
		0.06	0.23	0.29	0.92	0.55	0.76
	Avg:	0.04	0.147	0.253	0.95	0.71	0.79
(c)	Remaining Thickness (mm)						
	Avg:	.0020	0.117	0.170	0.97	0.77	0.86

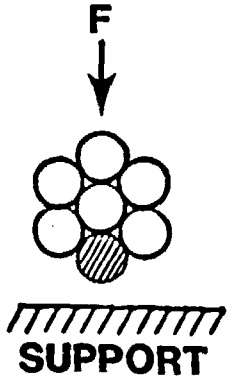

Nominal stress: 14 MPa
Exposure time: 1 day at 190°C

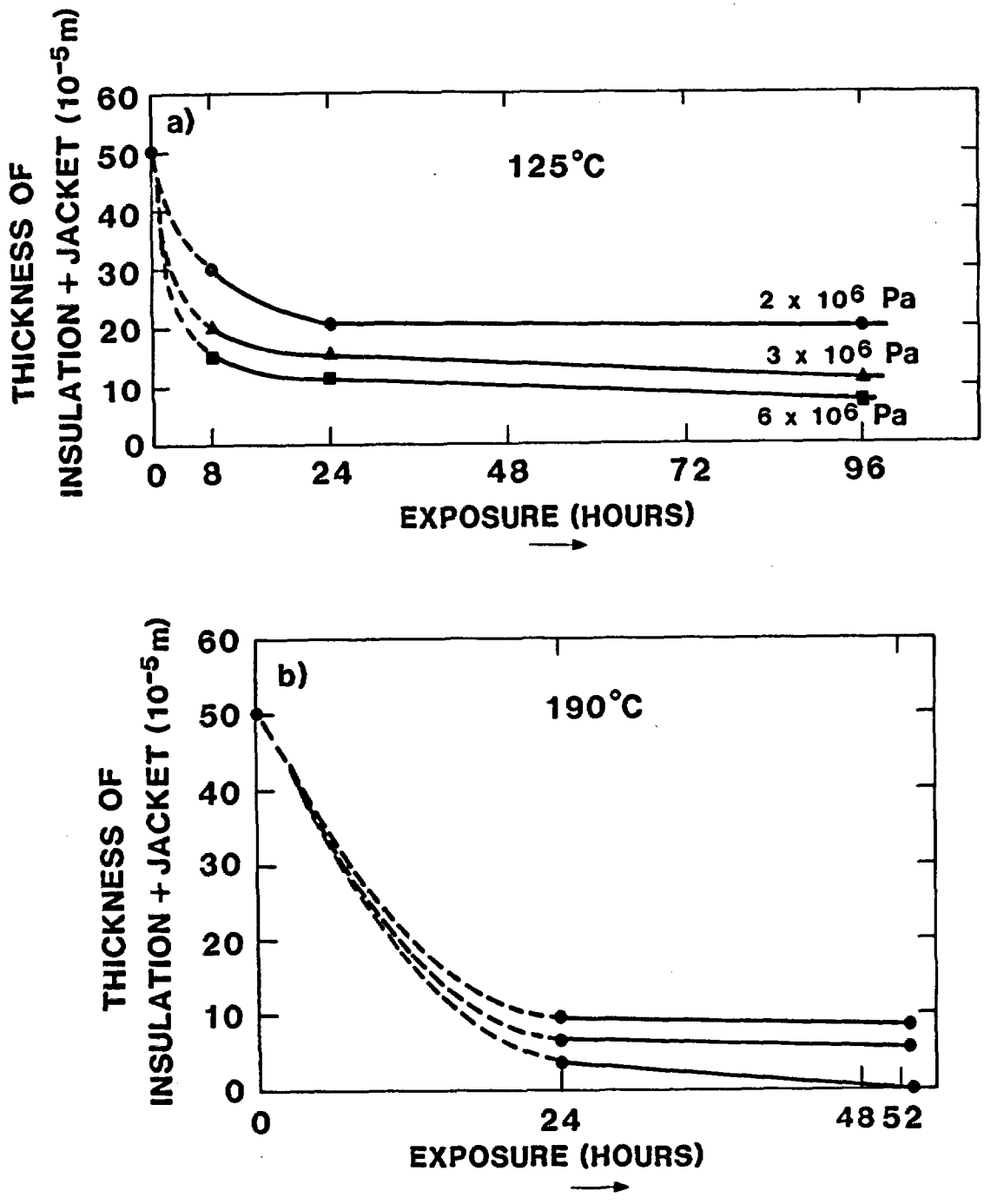

Figure 22. Creep Measurements at 125°C and 190°C

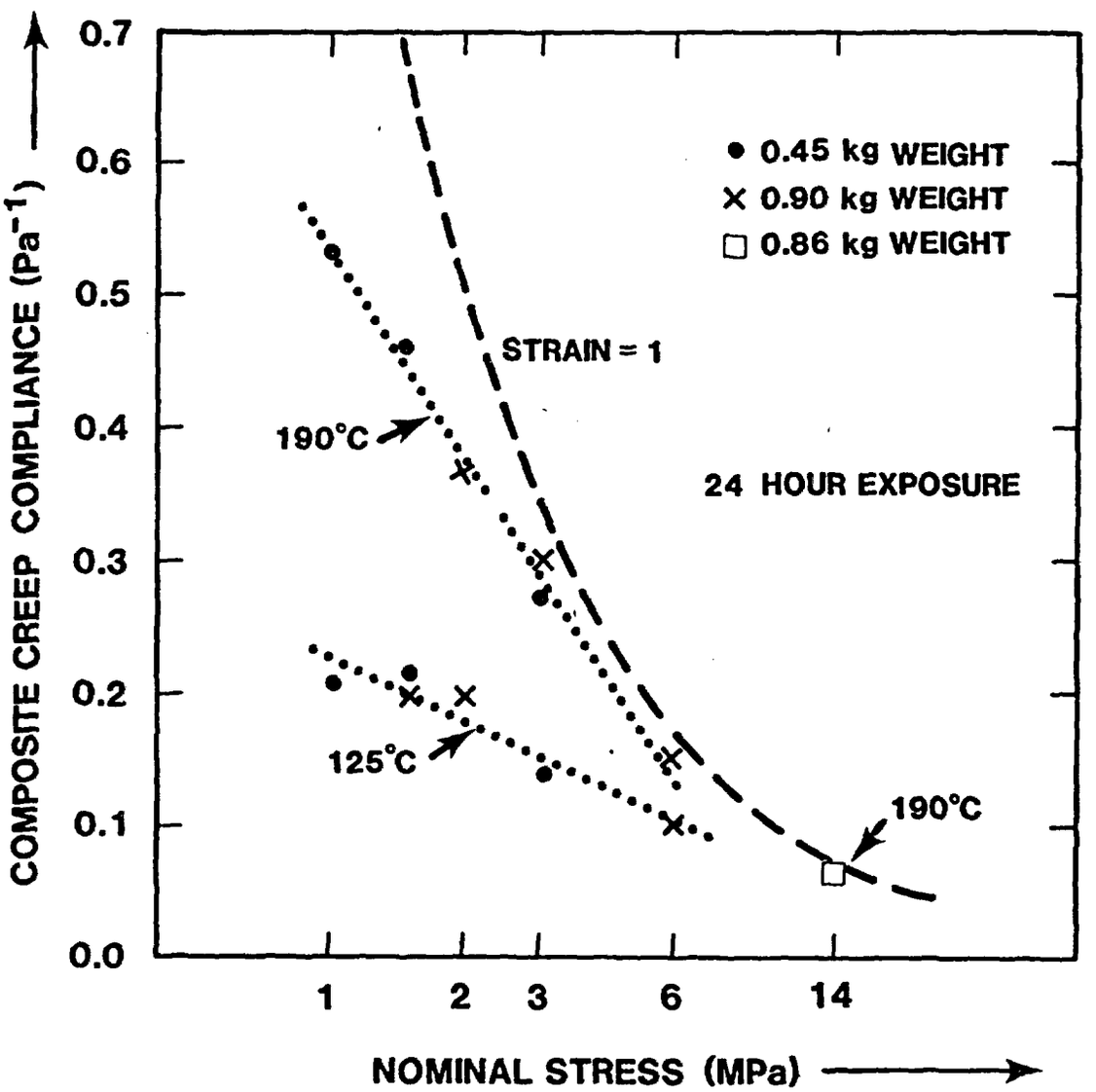

Figure 23. Creep Compliance vs Applied Stress for Various Exposure Temperatures

exact cause of the compliance decrease is (perhaps strain hardening or compacting). The phenomenon is beneficial because the lower compliance delays shortout.

Another probably related, and also helpful, phenomenon concerns breakdown fieldstrength. With the insulator and jacket thicknesses decreasing, the electrical breakdown voltage should decrease. This does not appear to be the case. As Figure 24 shows, breakdown voltages measured for 18 cables at 225°C do not vary significantly with the thickness of the remaining layer. The explanation for this may be that mechanical compression near the support improves the insulating material (e.g., by removing bubbles, closing microcracks, and densifying the polymers). Using an experimental facility developed by K. Gillen,[26] a 5% density increase was measured for EPR samples removed from a location just above the support point. Cable breakdown in the support region therefore becomes less likely with increasing exposure; breakdown along flaws at other locations remains unaffected.

A third phenomenon further decreasing the breakdown probability has been observed. Over long times, and probably affected by vibrations, the "unfavorable" wire strand position (shown in Table 3, (a)), appears to be unstable. The cable tends to twist towards the more stable position indicated at the bottom of Table 3. The wire now sinks in more slowly, and shortout at the support is delayed.

This work demonstrates the complexity of creep shortout. Long-term extrapolation from short-time tests is difficult under the circumstances.

3. Systematic Experiments

As a consequence of the considerations in Sections I and II and backed by results of the preliminary tests, a long-term experimental effort has evolved, which is continuing. The part pertaining to creep phenomena, particularly creep shortout, will be discussed here.

a) Program -- In the main test facility described in Section III, 6 experiments are being conducted in heat chambers maintained at 75°, 100°, 125°, 150°, 175°, and 225°C. A seventh experiment is taking place in the open at room temperature. In each test, creep versus time is measured by X-ray observation of the gradual reduction of insulator thickness in 6 cable samples. Each cable is hung over a 4.8-mm diameter steel rod and the cable-ends carry 0.45-kg lead weights. For three of the six cables in each test, an ac voltage of 480 V, between cable wire and support, generates an electrical field tending to pull cable wire and support together. The small mechanical stress of about 3 Pa (0.4×10^{-3} psi), which increases rapidly with decreasing distance, induced by the

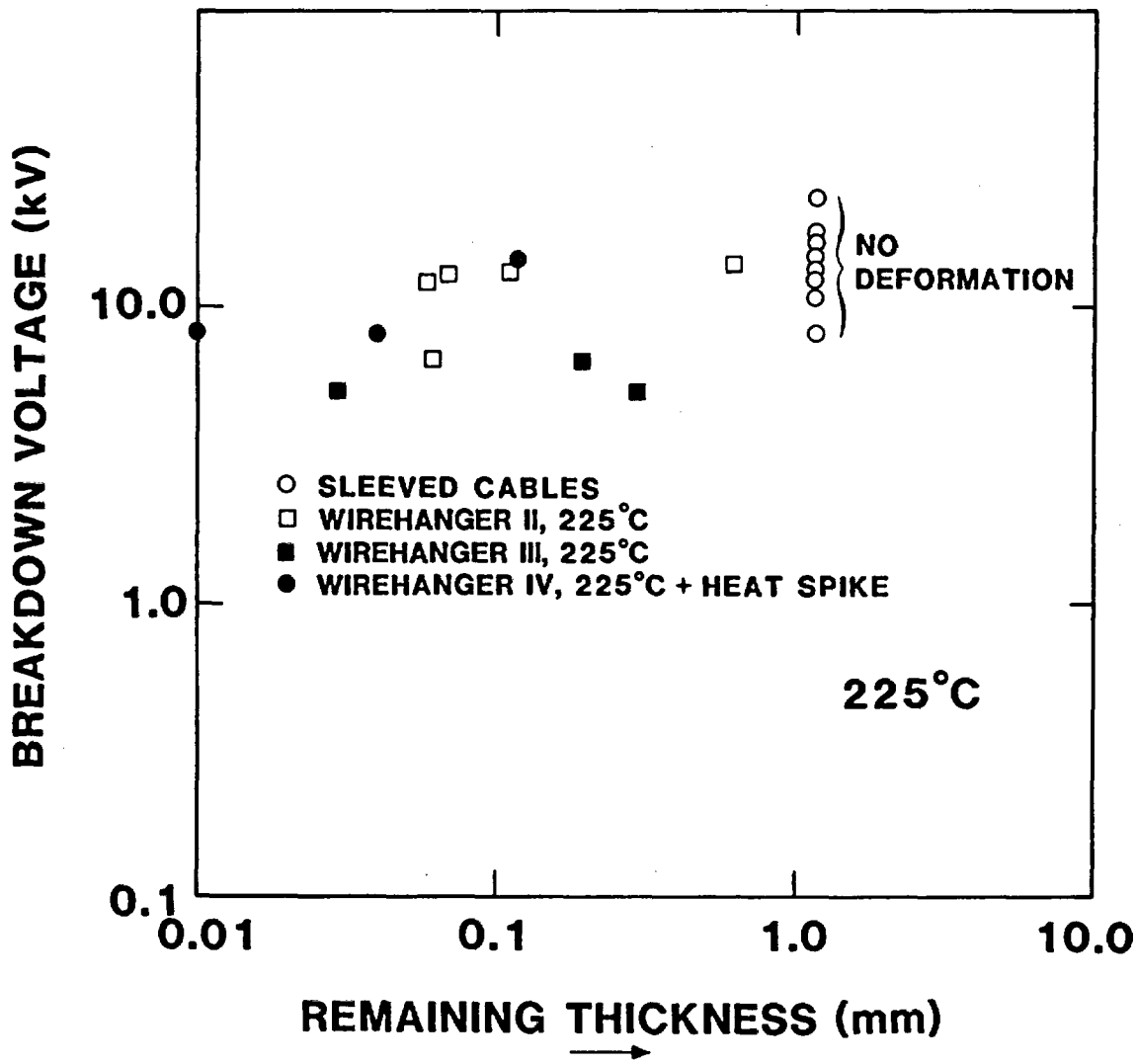

Figure 24. DC Breakdown Voltage vs Remaining Polymer Thickness at 225°C

voltage also causes 120 Hz mechanical vibrations. (Figure 10 shows one of the seven tensioning arrangements. Alignment and correction methods for the measurements have been described in Section III.)

b) Measurements -- Figure 25 shows an X-ray negative of the six bent cables on one of the cable tensioners. One of the bends is magnified five times in Figure 26 (positive) to show more clearly the calibration hole and the support area. The scalloped appearance of the wire shadow is due to the twisting of the seven cable strands, which leads to the effect tabulated in Table 3. In Figure 26a, the positioning of the cable on the support is symmetrical, the desired situation. In Figure 26b, the cable has slipped to the side and the shadow of the wire at the support point makes an angle, α, with the horizontal.

All measurements were made from negatives at a magnification of approximately 40. Figure 27 is an example. The projections of the thicknesses of the EPR and of the Hypalon were measured on a line drawn perpendicularly to the wire shadow, indicated by the line with arrow; this line is at an angle, α, with the vertical as explained above. The accuracy of the measurements is limited by the fuzziness of the boundaries. With experience, repeated measurements became reproducible. About 5% of the pictures were computer digitized, and a density trace was made along the measurement line (Figure 28). From these, thicknesses could be more accurately found. These precision measurements correlated to the standard measurements within 0.5 mm, which is equivalent to 12 μm in the actual cable samples.

Measurements were tabulated in the form shown in Table 4. The sample data in Table 4 were taken after 2-mo exposure at 175°C. The first nine rows of the table contain raw data and the other rows are computer evaluations as follows.

- Rows 2, 3, and 4 show the thicknesses in mm for the EPR and Hypalon layers, and the independently determined total insulation thickness, measured on the negatives similar to Figure 27.

- Row 5 lists the tilt symmetry angle, α, introduced in Figure 26, for possible later use in correlation.

- Rows 6, 7, and 8 use the support width, d, defined in Figure 27, and the major and minor axes of the elliptical projection of the calibration hole. Support width is known to be 4.76 mm, and the major hole diameter is very close to 1 mm. The two quantities are therefore useful to obtain scaling factors. In row 6 the scaling factor is printed out directly.

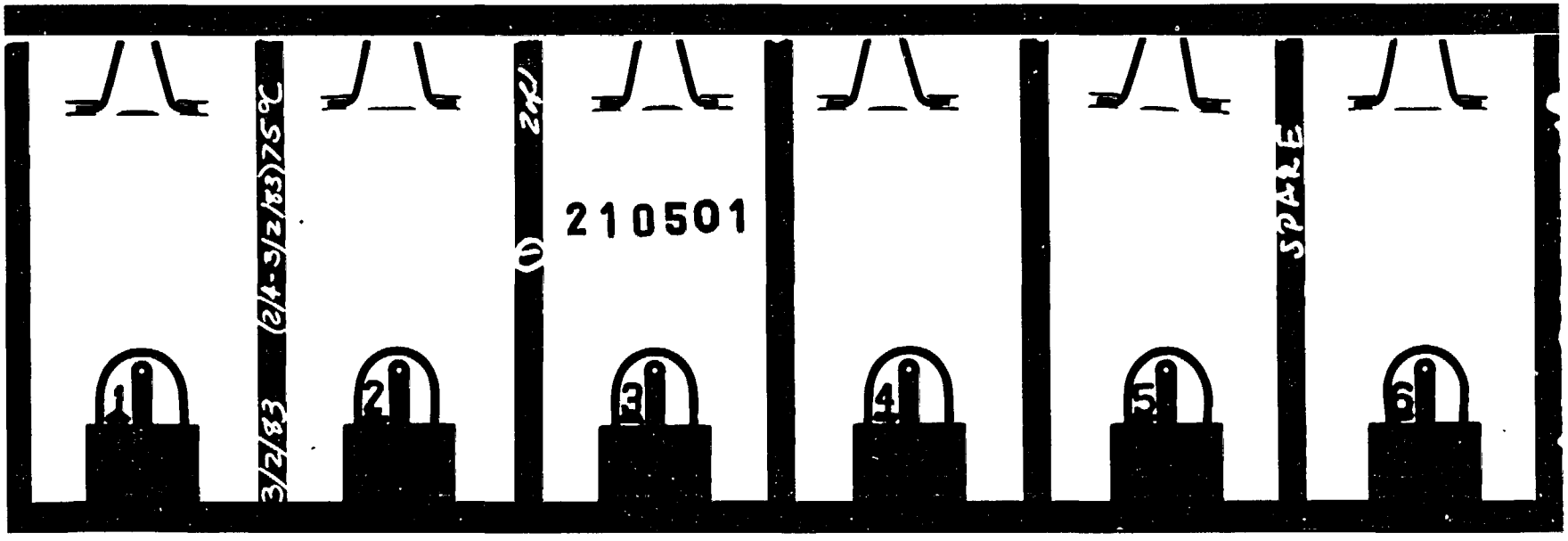

Figure 25. X-Ray Negative of Tensioner

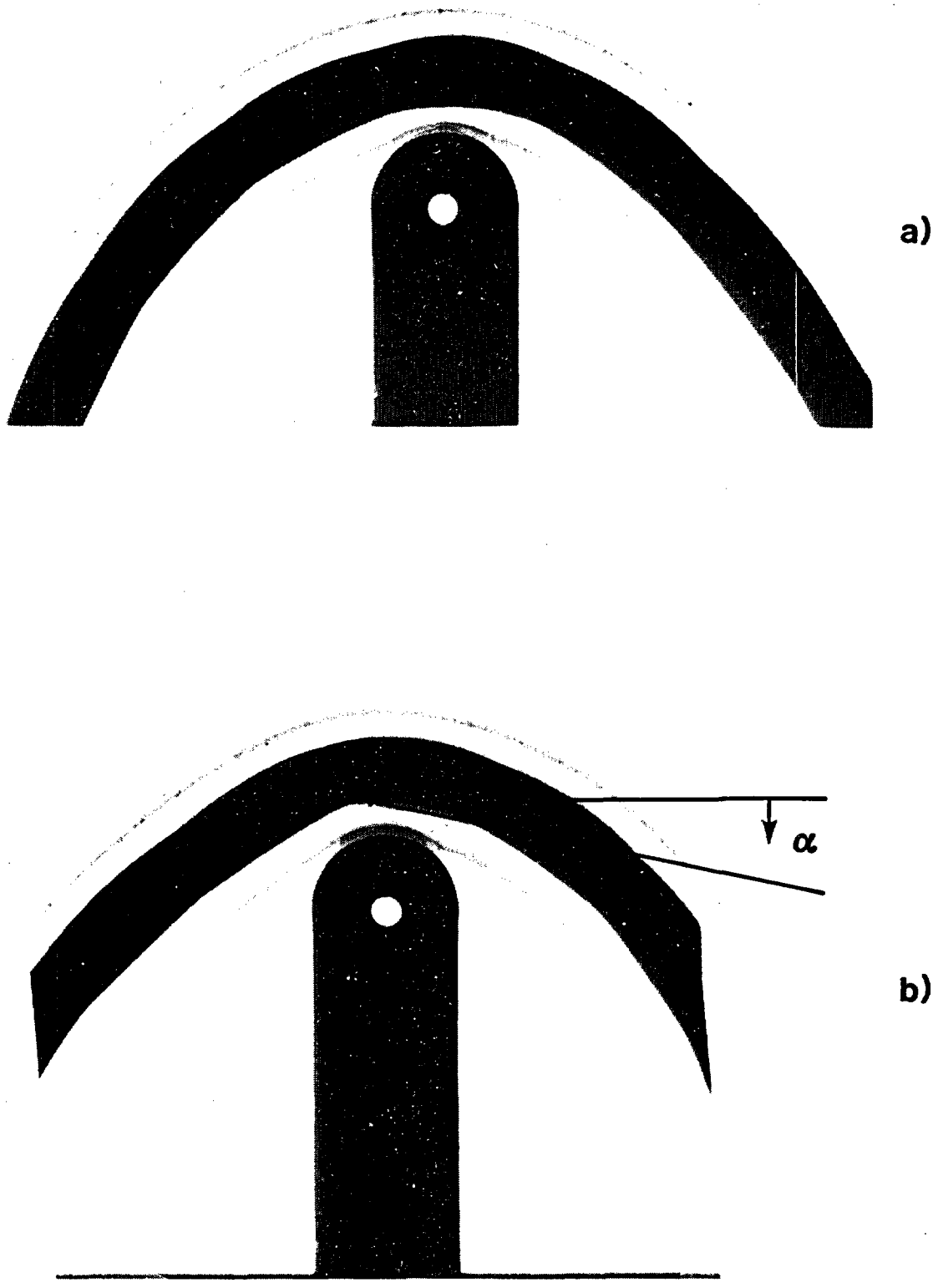

Figure 26. Symmetric (a) and Unsymmetric (b) Hang

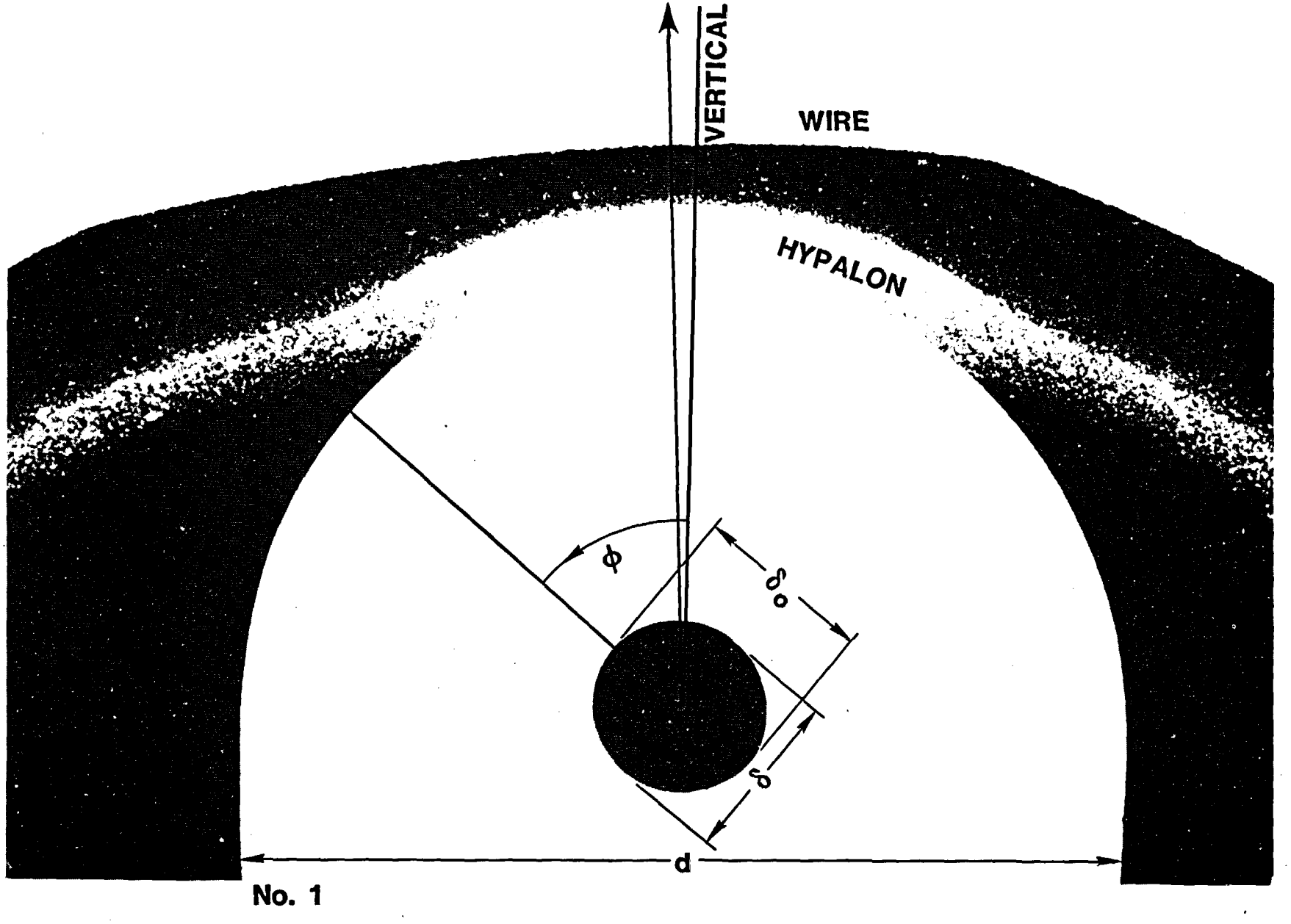

Figure 27. Measurement Parameters (38 x)

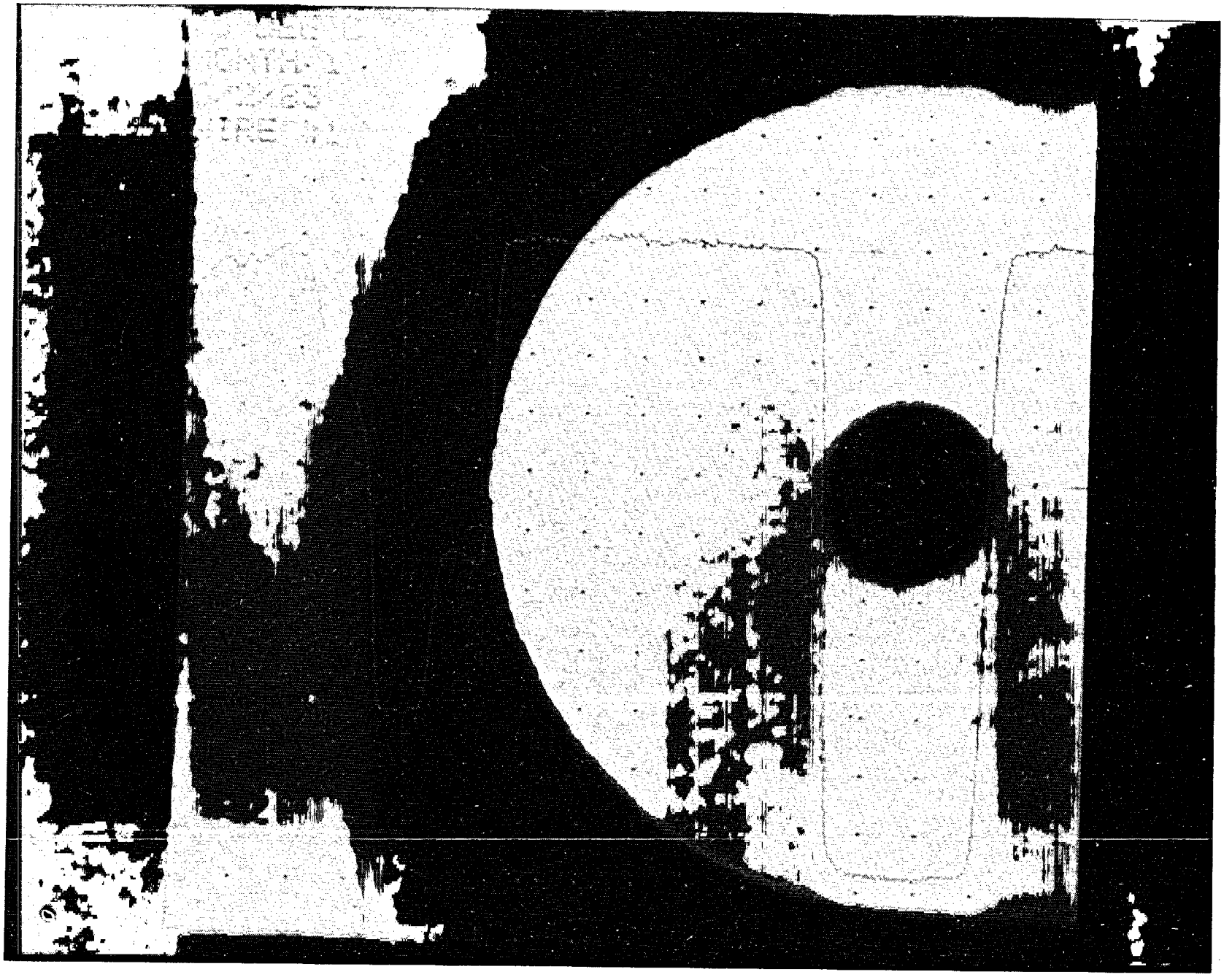

Figure 28. Density Distribution

Table 4

Example of Data Evaluation

Raw Data			175°C, 2-mo exposure			
1 Cable Number	1	2	3	4	5	6
2 EPR, measured (mm)	14.0	12.0	12.0	14.5	13.0	11.5
3 Hypalon, measured (mm)	9.0	10.0	10.0	10.5	10.5	9.0
4 Total, measured (mm)	23.0	22.0	22.0	25.0	23.5	20.5
5 Alpha, (degrees)	9.0	1.0	1.0	1.0	1.0	0.0
6 Support thickness (mm)	39.5	39.5	39.5	39.5	39.5	39.5
7 Large hole diameter (mm)	38.0	38.0	38.0	38.0	38.0	37.5
8 Small hole diameter (mm)	35.0	37.5	36.0	38.0	37.0	35.0
9 Phi, (degrees)	15.0	35.0	20.0	0.0	50.0	55.0
Computer Evaluations						
10 Kappa (µm)	23.7	3.9	15.8	0.0	7.9	20.0
11 K*sin(phi)	6.1	2.3	5.4	0.0	6.0	16.4
12 EPR (µm)	354.4	303.8	303.8	367.1	329.1	291.1
13 Hypalon (µm)	234.0	255.4	258.6	265.8	271.9	244.2
14 Total (µm)	588.4	559.2	562.4	632.9	601.0	535.4
		EPR		Hypalon		TOTAL
15 Average (µm)		324.9		255.0		579.9
16 Std. dev. (µm)		28.0		12.7		31.7
17 Deviation (%)		8.6		5.0		5.5
18 Reduced, EPR (%)	44.9	38.7	36.3	39.7	39.4	34.2
19 Reduced, Hypalon (%)	29.7	32.5	30.9	28.8	32.5	28.7
20 Reduced, Total (%)	74.6	71.3	67.2	68.5	71.9	62.8
21 Average, E,H,T (%)		38.9		30.5		69.4
22 Std. dev., E,H,T (%)		3.3		1.6		3.8
23 Deviation (%)		8.6		5.3		5.4
Group Averages						
24 E,H,T, 1..3 (%)		67.9		75.3		70.9
25 E,H,T, 4..6 (%)		64.5		72.4		67.7

- Row 9 gives the values for the measured tilt angle, α, versus the vertical, indicated in Figure 27.

- A computer program calculates corrections and averages of interest from the raw data. (The digit behind the decimal point in rows 10 through 14 is carried only for program convenience and is not significant.)

- Row 10 determines the support shadowing correction (see Figure 12) from the minor to major ellipse axis ratio, i.e., from the data in rows 6 and 7. The value is shown in microns.

- Row 11 improves the correction by taking the tilt angle (row 8) into account.

- Row 12 shows the actual thickness of the EPR layer in microns, calculated by dividing row 2 by row 6.

- Rows 13 and 14 list the corrected thicknesses for the Hypalon and for the total polymeric layers. As the lower part of these layers may be partially covered by the support, the correction calculated in row 11 is added.

- Row 15 provides averages for the 6 thickness measurements in rows 2 to 4 in microns. The EPR values are listed in column 2, Hypalon and total values in columns 4 and 6, respectively.

- Rows 16 and 17 contain the standard deviations for row 15, in microns and percent, respectively.

- In rows 18 to 23 are listed the normalized values for the data presented in rows 12 to 17; for each cable the total thickness before exposure is defined to be 100%. The normalization will be discussed below.

- Finally, in rows 24 and 25, reduced group values are listed. These help in assessing differences between the three cables under voltage and the three non-energized cables. Here the preexposure thickness for each of the layers is set at 100%.

The reason for introduction of normalized values is that the original dimensions of the cable samples, although taken sequentially from the same reel, vary severely. Bending the cables over support rods increases the variation. In Table 5, some statistical data of interest are shown. The first three groups of figures show before-exposure averages for all 42 cable samples used in the creep experiments; thicknesses and standard deviations are measured in microns and the

Table 5

Preexperiment Averages

All EPR	552.8
Standard deviation, EPR	55.3
Standard deviation (%)	10.0
All Hypalon	328.7
Standard deviation, Hyp.	35.2
Standard deviation (%)	10.7
All cable	881.6
Standard deviation	69.4
Standard deviation (%)	7.9
Reduced thickness, EPR, (%)	62.7
Standard deviation (%)	3.4
Standard deviation (%)	5.5
Reduced thickness, Hyp., (%)	37.3
Standard deviation (%)	3.2
Standard deviation (%)	8.6

relative standard deviations in percent. For a population of 42, a standard deviation of 10% must be considered large. Normalization of the total thickness to 100% eliminates the standard preexposure deviation for this parameter; as the two bottom groups in Table 5 show, the deviation for the EPR insulator is halved, and the deviation for the jacket somewhat improved. The original dimensions are therefore not distorted proportionally. This points to nonuniformity of composition or of processing and makes extrapolation more difficult.

c) Preliminary Results -- This investigation attempts to extrapolate a few years of data to the 40-yr service life of cables in a reactor containment. A suitable form for discussing such an extrapolation is the log-log plot of remaining thickness versus times shown in Figure 29. The indicated power curve is a straight line which conveniently drops uniformly from 100% to 1% in 40 years. A reduction of the total insulation thickness to 1% means that about 10 μm of insulator/jacket material would remain between wire and support. From Figure 24, it is seen that a breakdown at this thickness is unlikely even for a potential difference of several kilovolts, and much more unlikely at operational voltage. If the measured thickness stays above this line, we may assume that creep shortout will not occur. In Figure 29, the remaining cable thickness, averaged over six cable samples, is plotted for the first few months of data. Some measured points are connected by curves. We expect thicknesses to gradually decrease as the EPR creep-modulus curves in Figure 17 indicate. This is usually observed. A slightly positive slope sometimes occurs as, for example, for the 75°C values. This is probably due to twisting of the cable sample, as the wire strands seek a stable position. Notice that the greatest reduction in thickness occurs for the samples exposed at 125°C. Such a worst temperature is expected because the materials first soften with temperature, but enhanced crosslinking at still higher temperature embrittles the polymers and retards creep.

In Figure 30 (a worst case) the thickness reduction situation is presented. Instead of the average, the cables with the smallest remaining thickness (out of the sample of six) have been selected. Again, the smallest remaining thicknesses occur for the 125°C experiment. The measurements do not tend to approach the critical curve defined above.

Creep compression of the EPR and Hypalon layers are not proportional; EPR is softer and contributes most of the combined creep strain. Figure 31 shows worst-case EPR thickness-reduction percentages. The 225°C values have the tendency to approach the critical curve. An explanation is that the squeezeout of the insulator (see Table 3) may be very rapid in the beginning before embrittlement slows the process.

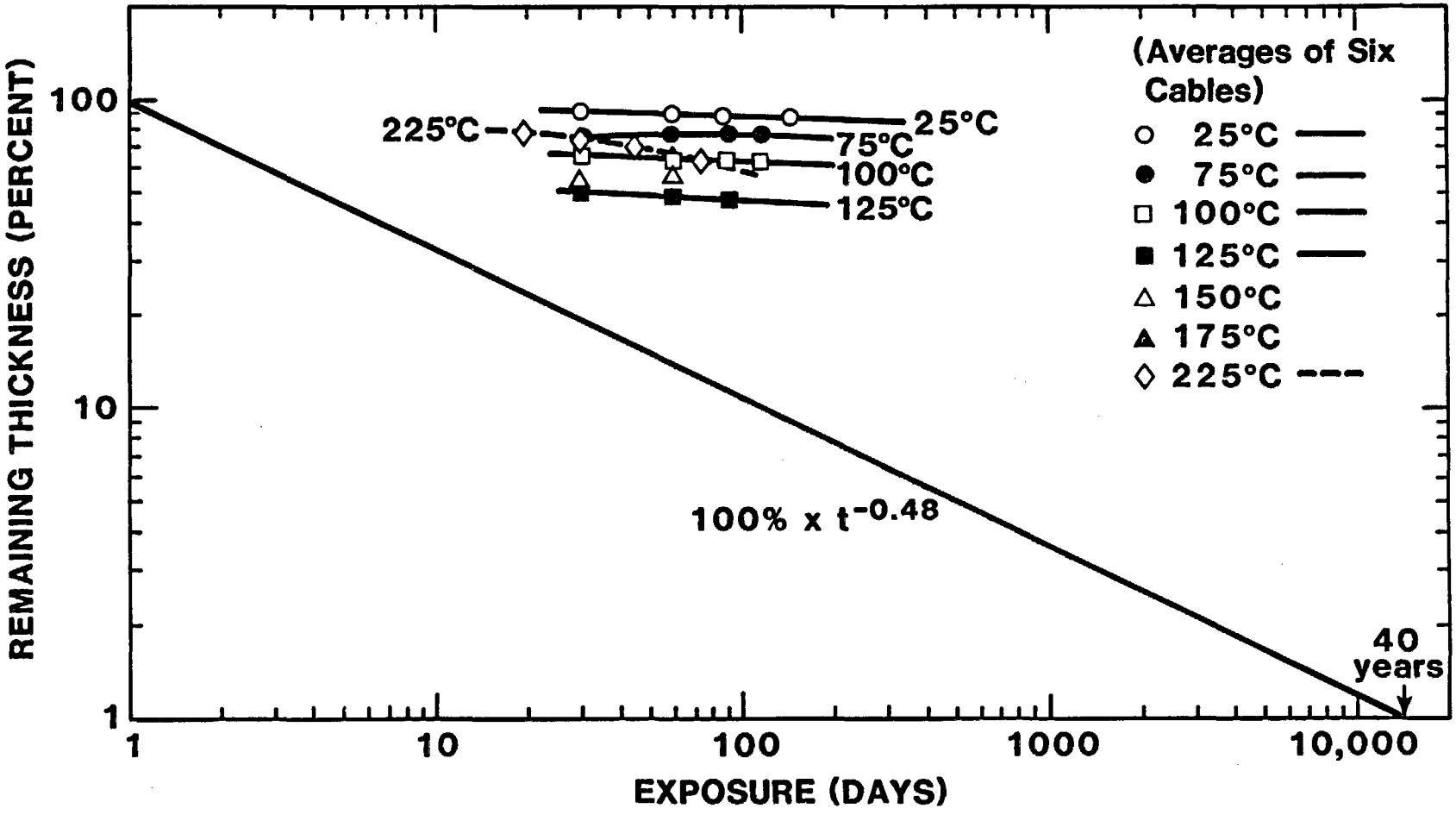

Figure 29. Average Reduction for 6 Cables

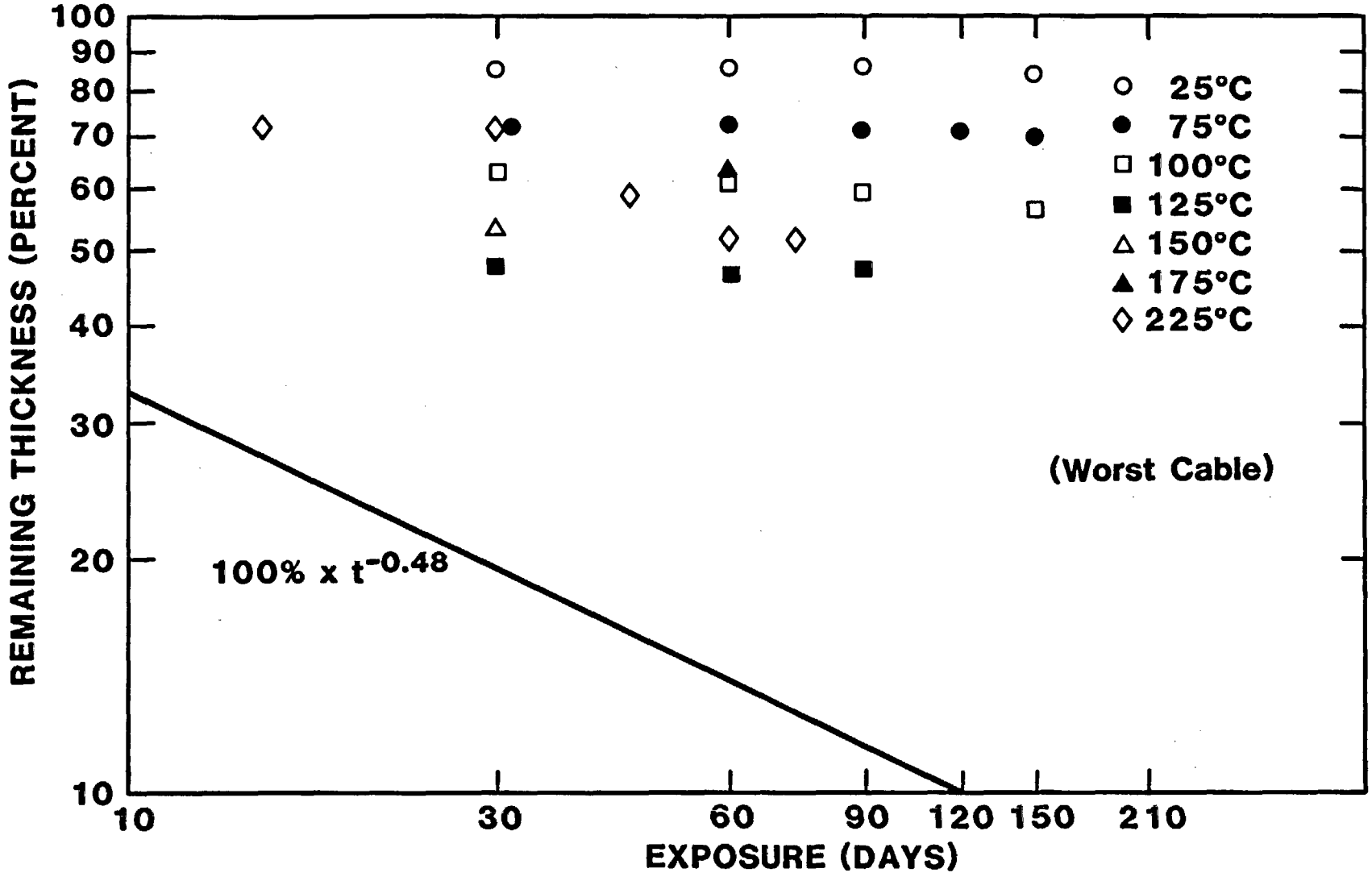

Figure 30. Thickness Reduction for Worst of 6 Cables

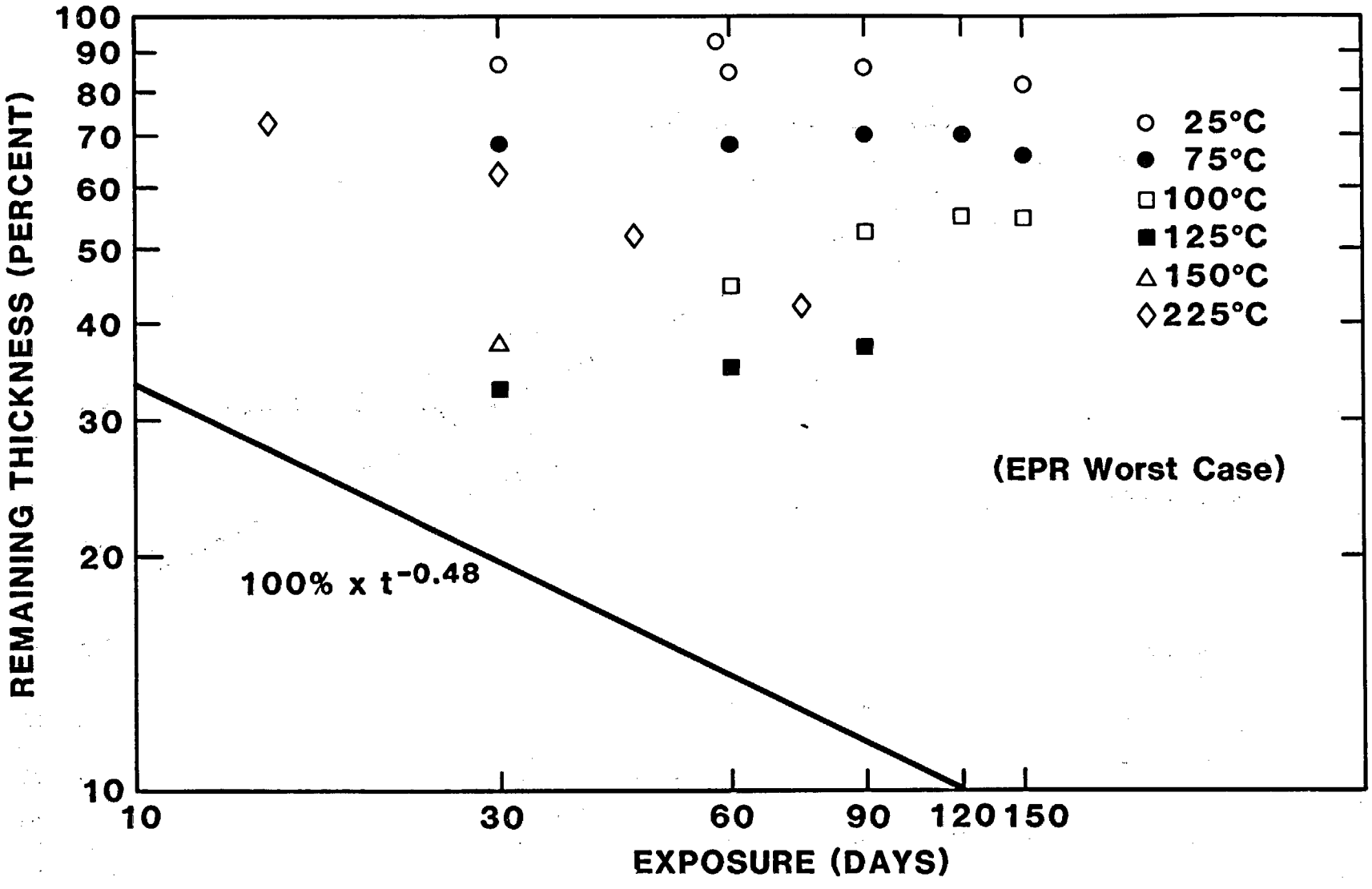

Figure 31. Worst Thickness Reduction for EPR Layer

With time, the polymeric materials tend to become more and more embrittled and the creep modulus increases; the creep curves in Figures 29 to 31 will flatten out and bend away from the critical curve. This leads to the expectation that at the tension load used in these measurements, shortout will not occur. This will be true if compression creep does not exhibit the nonlinearities well known for tensional and torsional creep. While this is physically unlikely, experimental proof is still required.

The above argument pertains only to actual creep shortout where all polymeric material has finally been squeezed out between wire and support. Other phenomena may occur for this geometric arrangement. It was observed in the 225°C test that the three cable samples under 480-V leads developed temporary electrical shorts, while severe cracking in the support neighborhood occurred. This situation will be discussed in Section V.

V. CRACKS IN CABLES

1. General Comments

Cracks in the insulator-jacket protection of a cable may lead to electrical shortout, especially during an accident when the combination of humidity, contaminants, and spray may form conducting paths to ground or to another crack.

Experiments have been performed during this investigation that show that the existence of a crack through jacket and insulator does not always lead to an immediate shortout, even if the cable is immersed in a conducting liquid. The conditions under which a short does not occur, even though cracks are present, are very complex and not completely understood. For the present discussion a criterion will be that cracks penetrating to the inner conductor may cause a shortout and are considered as a "failure".

Three specific situations are of primary concern:

a) Long cables lying in conduits or trays may develop cracks under thermal cycling; it is believed that shrinkage of the polymers with temperature and time is associated with the cracking.

b) Cables, sharply bent, (e.g., around conduit corners) may crack under the mechanical stress produced by temperature cycling or by overhang weighting.

c) Cables, embrittled by aging, may be mechanically stressed and cracked by "maintenance" procedures.

Variations and combinations of these characteristic situations may occur.

The investigation of cracks in cables is made difficult by two phenomena. First, a crack will originate at a surface flaw, and the distribution of surface discontinuities is generally widely variable; once a crack starts enlarging, it relieves tensional stresses in its neighborhood and prevents further cracking there. Second, cracks, especially small ones, can heal again.[29] Measurements of number and size of cracks occurring for a certain temperature history and stress distribution will show large variation.

Investigations at the Bell Telephone Laboratories[30] have shown that for LDPE cables the time needed to develop incipient cracking, plotted versus inverse temperature, exhibits non-Arrhenius behavior. It cannot be assumed that the present materials combination behaves more simply.

2. Preliminary Tests

a) Long Cables -- It is of interest to learn if and when long cables, lying undisturbed in a conduit and under a minimum of stress, can develop cracks. In a pipe arrangement similar to the one shown in Figure 7 and discussed above, a bundle of six, parallel, 10-m-long cables were gradually heated over a 2-h period by cable current to a temperature slightly above 300°C. The test simulated a severe overload condition. After cooling it was seen that the cables clamped at the ends of the long pipe had warped and some had crossed over the others. Both perpendicular (circumferential) and longitudinal (axial) cracks were found (see Table 6). The perpendicular cracks penetrated through both jacket and insulator; the axial cracks occurred in the jacket only. A subsequent test at a much lower temperature of 90°C, but otherwise identical, did not produce any cracks in a 10-month exposure.

Perpendicular cracks are not easy to explain. For a crack to occur, a tensional stress perpendicular to the direction of the crack must be present. This stress cannot be generated by the thermal expansion of the steel pipe, as the expansion coefficient for both copper wire and for the polymeric insulation are larger than the coefficient for steel. The cooling cycle cannot be responsible, since it was observed that at least a part of the cracks occurred before the system cooled down. A possible explanation may be the shrinkage of the polymeric materials.

A number of experiments with a specially developed precision-volume measuring device demonstrated the following behavior for cables exposed to increased temperature. The polymeric material's specific volume increased due to the the positive thermal-expansion coefficient of the polymeric material (see e.g., Ref. 15, Figure 3-7). After hours or days in the temperature range of interest, loss of material due to chemical decomposition decreases the volume. The final volume loss increases with temperature, approaching a saturation value with time; a 15% decrease was measured for a several-day exposure of the cable to 185°C.

Assuming a (worst case) three-dimensional uniform shrinkage of 20%, a strain of less than 0.07 would be generated. According to Equation 1, using a high-temperature modulus of 2070 kPa (Ref. 15, Figure 5-3), a stress of 145 kPa would exist, which could gradually open a crack. The present geometry does not have three-dimensional symmetry, however. In fact, for an infinitely-long uniform cable no axial tensional stress would develop. As severe perpendicular cracks do occur, an axially nonuniform stress distribution must exist. Bends in the cables do provide asymmetry. A more likely condition is nonuniform "sticking" of the cable insulator to the

Table 6

Crack Statistics After Heating to 225°C Over 5 Days

Experiment	I	II	III	IV
Number of cables	10	10	10	5
Load per cable (kg)	1.6	0.34	0.34	0.34
Environment	Dry	Dry	Humid	Humid (Heat Spike)
Average number of cracks per cable	4.6	1.9	2.3	1.6
Standard deviation	40%	34%	21%	154%
Average width of cracks (mm)	0.9	1.1	1.6	0.1
Standard deviation	27%	51%	42%	----
Integral crack width (mm)	4.2	2.1	3.7	0.16 (Est.)
Insulator cracks (percentage)	77%	35%	67%	0

cable wire; this phenomenon has often been observed when cooled-down cables are disassembled.

Cracks parallel to the axis are generated by circumferential stresses. Measurements have shown that the outer Hypalon jacket tends to shrink more than the inner EPR material. This enhances the circumferential stress and may explain why parallel cracks almost always occur only in the jacket and do not penetrate the insulator.

b) Cracks in Stressed Bends -- In this test, 35 cable samples made of EPR/Hypalon were exposed to a thermal treatment in which the temperature was slowly increased over a period of 5 days to 225°C in steps of 25°C. The cables were stretched over a sharp edge with weights of either 1.6 kg or 0.34 kg each. Half the experiments were performed in a dry atmosphere; for the other half, the humidity ranged between 95% and 100%. In the last experiment, a one-hour heat spike of 265°C was applied before the normal heating sequence.

Listed in Table 6 is the average number of observed cracks, the average width of the cracks, and the integrated crack width per cable. Also given is the percentage of cracks which reached the conductor (through cracks). It was observed that the formation of cracks increased strongly between 200°C and 225°C. The cracks were formed and counted before the system had time to cool noticeably. Some cracks may have deepened in the subsequent cooling period. One crack in experiment III was found to have healed after cooling.

The most severely stretched cables, those in experiment I, clearly exhibited the largest number and the highest total width of cracks. It is not clear why the average crack width was very low in this experiment. The presence of humidity during the relatively brief aging experiments does not seem to have noticeable influence. The addition of a heat spike, simulating a temporary overload, had strong impact. It resulted in very tiny cracks (or crazing) which did not penetrate to the conductor. This inconsistency (and some of the observations above) may be related to the adhesion of the insulator to the center wire. In the first three experiments, the three cable components (jacket, insulator, wire) stuck inseparably to each other after cooling. The heat spike in test IV led to easy separability of the three.

c) Maintenance Accident -- The many data in literature describing the influence of temperature and radiation exposure on materials properties have almost always been taken after cooling to room temperature. The results therefore may not be descriptive for what happens at high temperature, but should be applicable for correlation with crack generation at room temperature, i.e., during "maintenance handling" of aged cables. A "maintenance accident" was simulated by bending cable samples around a mandrel. The mandrel diameter was

usually approximately equal to that of the cable; this certainly constitutes a severe overtest.

Cracking will occur if the breaking strain or "elongation to rupture", e, of the deteriorated polymer is exceeded. A simple two-dimensional model for estimating strains on the outer surface of a bent cable can be developed with the help of Figure 32. A strip of cable material of width 2ρ is bent (without deformation of the cross section) over a cylinder of radius r. At the outer side of the geometry, where cracks can start developing, the length of the plastic around a quarter bend is $\pi(r + 2\rho)/2$. At the neutral fiber, the corresponding length is $\pi(r + \rho)/2$. The resulting bending strain is then $\rho/(r + \rho)$. This strain is augmented by σ/M, if an applied stress, σ, exists, where M is the appropriate modulus. Cracks will develop if the sum of these strains exceeds or equals the breaking strain, e, that is, if

$$e \leq \frac{\rho}{r + \rho} + \frac{\sigma}{M} . \qquad (4)$$

In experiments performed with cables and not with strips of material, pure bending without pulling was attempted with a jig similar to the one in Figure 13. Stress, σ, was taken to be zero. It was assumed that the effects caused by potential sticking of the polymeric material to the center conductor were negligible. Lateral deformation of the geometry (usually less than 10%), was also neglected. The model cannot take into account the (ever-present) flaws in the material; presumably, the value of e accounts for this on a statistical basis. Considerable scatter in the measured data is to be expected.

For the cable used, ρ for the Hypalon jacket has an average value of 2.4 mm, and for the insulator, 1.9 mm. If the cable is bent over a 4.8-mm-diameter mandrel ($r = 2.4$), strains of 0.5 and 0.4, respectively, are created. It is customary to normalize strain values to the original room-temperature breaking strain, e_o, which is about 3.5 for these materials. Cracks should therefore become likely when e/e_o equals 0.15 for the jacket (Hypalon) and 0.10 for the insulator (EPR).

In Figure 33, the time needed for EPR and for Hypalon to reach the values $e/e_o = 0.10$ and 0.15, respectively, is plotted versus inverse temperature. The data are extrapolated from Reference 31 and supported by Sandia measurements on similar EPR and Hypalon compositions.[26] The extrapolation is justified in Reference 22. Five standard cables were aged at 186°C for 8, 16, 32, and 48 hours and for longer periods. As indicated in Figure 33, the jacket exhibited cracks after 32 hours. The insulator did not crack until after 300 hours. The experimental results are certainly compatible with the model developed.

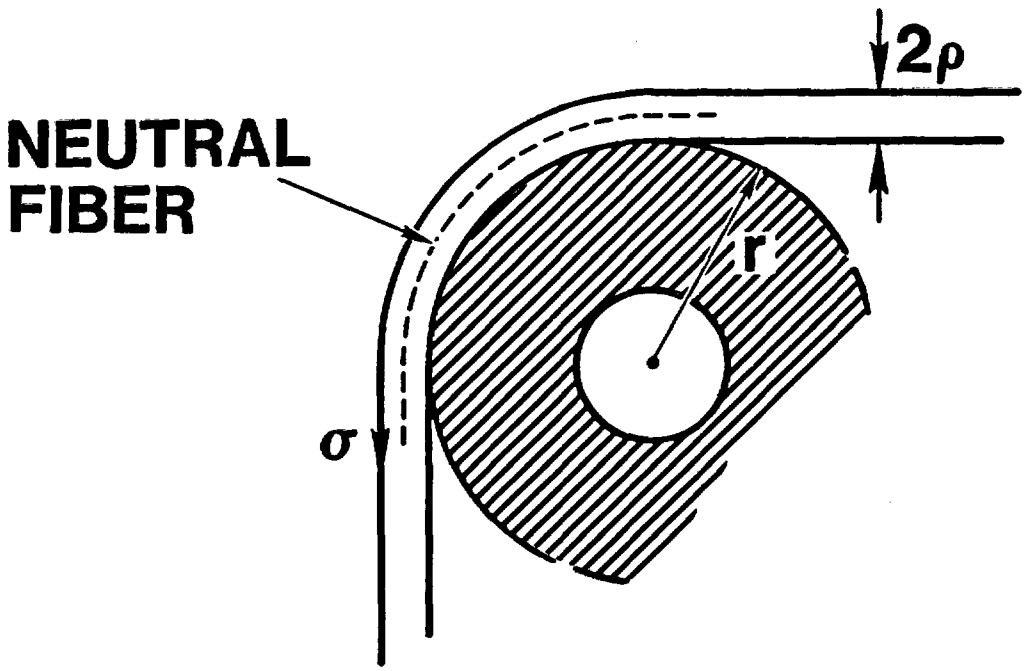

Figure 32. Model for Equation 4

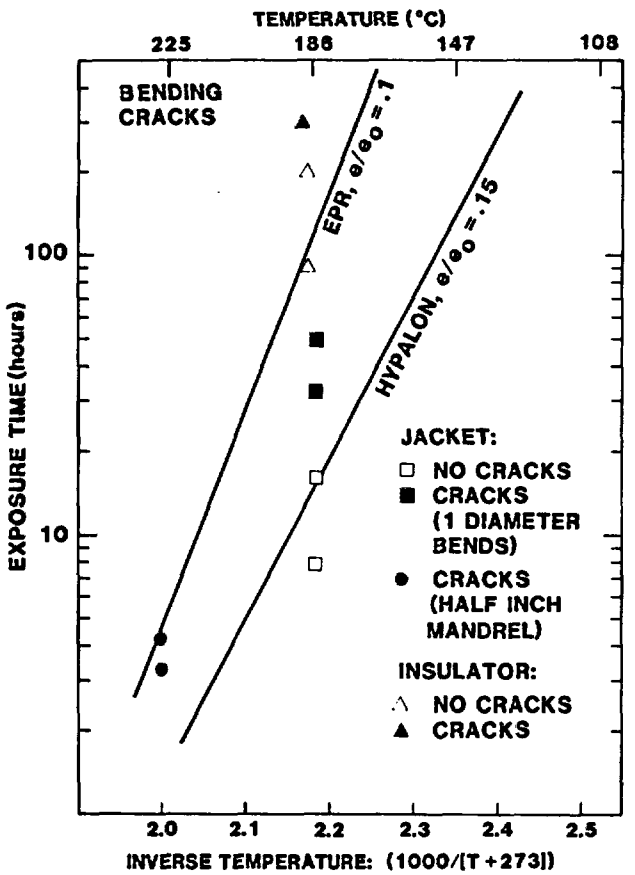

Figure 33. Crack Experiments

Some earlier observations for a 225°C exposure are also indicated in Figure 33. During the experiments I through III described in connection with Table 6, straight as well as prebent cables were exposed to temperature treatment with no axial stress applied. The cables remained a few hours at 225°C and were then bent (or unbent) after cooling. The bending radius was 6.4 mm in these experiments. According to Equation 4, cracking should occur for $e/e_0 = 0.08$ (Hypalon) and 0.06 (EPR). The graphs for these values would lie just above the respective plotted lines in Figure 33. Jacket cracks were observed as shown. The insulators did not crack because the exposure did not last long enough.

The results indicate that a basic understanding for cold cracking of cables exists, at least if embrittlement has been achieved at high temperatures and therefore in short times. For extrapolation to long-time behavior, more precise and more systematic tests are needed.

The model based on Equation 4 may be useful to estimate the embrittlement ratio e/e_0, above which no cold cracks will occur. For a very sharp bend (kink), the bending radius r will be very small and the ratio $\rho/(r + \rho)$ will tend towards unity. With $e \sim 1$, the limiting value e/e_0 for the materials used in the experiments described above will be about 0.3. A very conservative working hypothesis would therefore demand that e/e_0 be kept above 0.4 to avoid cold bending cracks. In the present experiments, no cracking has been observed above this value.

3. Ongoing Systematic Tests

a) Dynamic Cracking -- The test series presently in operation makes use of available space in the heat chambers used for the creep tests described in Section IV. Cable samples are being aged at 75° to 175°C in intervals of 25°C, and at 225°C. Every month, and semimonthly for the two highest temperatures, the heating cycle is interrupted and the cables are permitted to cool down so that samples for crack tests can be withdrawn. The samples consist of 0.2-m-long straight pieces of cable lying on the bases of the creep tensioners (Figure 10) and/or on the floor of the heat chambers. In spite of fan circulation, small heat gradients exist on the heat chamber floor and the samples are not all at precisely the same temperature. At the end of the test series, the straight vertical pieces of the creep test specimens will be used for crack tests.

After removal the samples are bent in the jig shown in Figure 14, and the cracks are counted. There are always many more surface cracks observed in the Hypalon layer than cracks extending through to the wire (through cracks). Also, perpendicular cracks outnumber parallel cracks. Data obtained up to now are plotted in Figure 34. Groups of 6 samples were

taken from the heat chambers at the indicated times, bent and analyzed. Shown in the graph are the number of through cracks, with perpendicular cracks in the top graph and parallel cracks at the bottom. Figure 34 shows that, for 225°C exposure and bending over a 12.7-mm mandrel, through cracks appear before one month of exposure. At 175°C, through cracks appear at about a month. The number of cracks grows rapidly with time. Data for the 150°C exposure are still too few to exhibit a clear trend. At still lower temperatures no cracks have yet occurred. As expected, the scatter in the data is substantial.

The cracking model predicts that an e/e_0 ratio of 0.04 or less is needed for cracks to start in the EPR layer, i.e., for through cracks. In Figure 33, the $e/e_0 = 0.04$ line would lie somewhat above the plotted 0.1 curve. The starting times for cracking at 225°C and 175°C taken from Figure 34 are compatible with the model plot in Figure 33.

b) Static Cracks -- As reported in Section IV, all 225°C creep experiments under voltage shorted out temporarily after an exposure of 2.5 months. The X-rays (see example in Figure 35) show striations not present in other pictures; in addition, the Hypalon layer has lifted off the support. The striations appear to be associated with cracks.

Inspection of the samples reveals that after the long, high-temperature exposure the polymers are completely embrittled. Temperature cycling, mechanical vibration naturally present and caused by the ac field, and asymmetric stress distribution lead to cracking. It is suspected that during the cracking process vapors and fluids in polymer pockets are freed and permit a surface breakdown discharge[32] along the crack walls. The discharge cleans the contamination and the insulator is functional again. Further observations are needed to verify this explanation. Repetition of the 225°C experiments is planned.

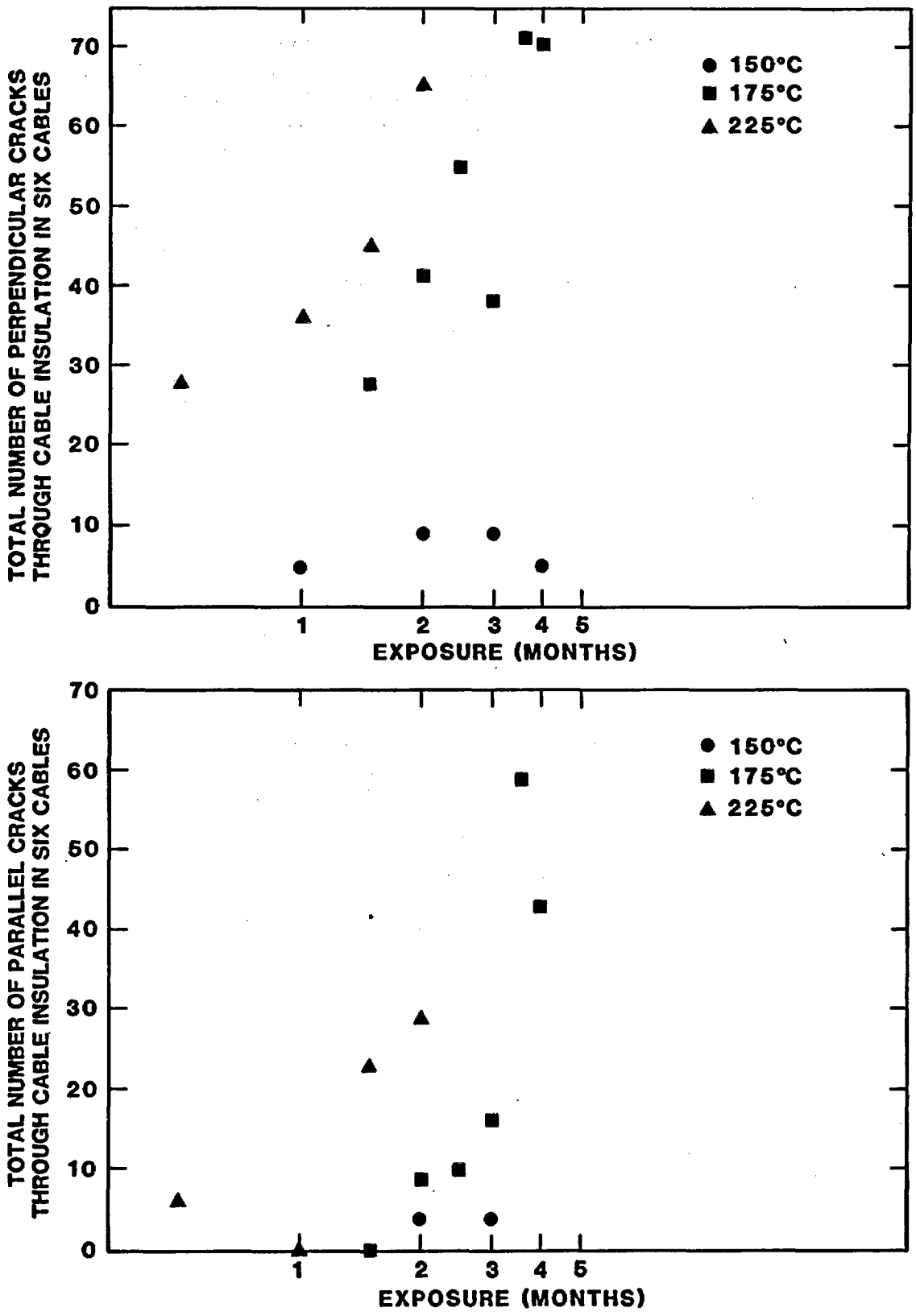

Figure 34. Total Number of Bending Cracks for 6 Cables vs Time

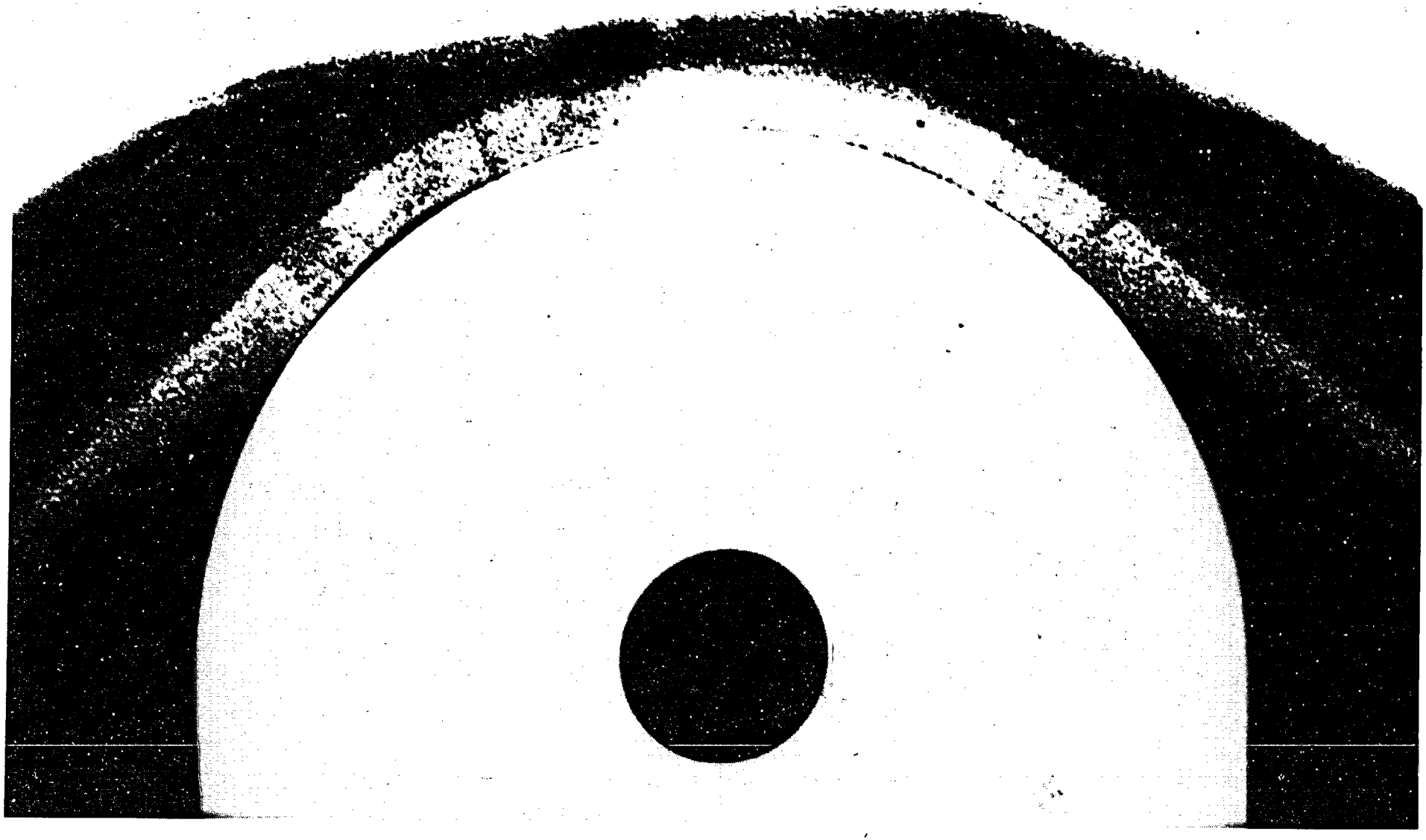

Figure 35. Embrittlement Cracks at 225°C

VI. CONCLUSION

The work is planned to continue, to generate more accurate bases for extrapolation and to obtain enough data to develop some scaling laws. Some preliminary results of the investigation can be given if the following assumptions are made:

a) There are no severe inherent flaws (e.g., metal chips) in the organic material.

b) No synergistic effects, other than those already observed in materials aging, will be found.

c) No chemicals other than water or watery electrolytes are present.

d) No strong mechanical vibrations will occur to shake embrittled insulation off the cables.

e) Cables are operated within current and voltage specifications.

Under these assumptions, operability approaching 40 years is to be expected for EPR - Hypalon cables, with the following limitations:

f) The cable temperature does not exceed 190°C (above this temperature thermal runaway may occur).

g) Cable overhang over edges with 3-mm radius of curvature must not be longer than 10 m and, for 6-mm radius of curvature, not longer than 30 m (creep shortout critical dimensions).

h) High temperatures do not last so long that cracks form in mechanically unstressed cables (long-exposure crack threshold).

i) Cables for which any combination of thermal and radiation aging has led to a breaking strain ratio (e/e_0) of less than 0.4, must not be handled or be permitted to move (bending crack threshold).

The last limitation is quite severe. If the Arrhenius model for embrittlement holds, the critical value as defined would be reached in 40 years at a containment temperature of 80°C with no radiation present. There is evidence, however, that this projection is very optimistic.

A number of installation provisions, which will mitigate or eliminate certain failure modes, recommend themselves:

(1) Insulating (instead of metallic) caps on conduit corners will eliminate creep shortout to ground; so will mechanical load relief (tying) for downhanging cables.

(2) Conduits could be completely filled with cables, or the cables could be tied, to prevent warpage.

(3) Sharp bends, prohibited by many installation specifications, must be avoided.

(4) Materials combinations in support structures, with vastly different coefficients of thermal expansion which could tension cables during thermal cycles, must be avoided.

(5) Sealed conduits and connection boxes are useful in preventing conductivity carrying or generating fluids from reaching cracks.

(6) Reliable circuit breakers will prevent overload damage.

REFERENCES

1. H. F. Reisinger, "Component Failures in Pressurized Water Reactors," Combustion Engineering Inc., Sandia Corporation Contractor Report 13-6442.

2. W. F. Lindsay, Science Applications Inc., personal communication.

3. M. B. Murphy, Sandia Laboratories, personal communication.

4. B. E. Bader, et al., "Proceedings of Workshop on Nuclear Power Plant Aging," NUREG/CP-0036, November 1983.

5. R. Grüb and B. Langeset, "Voltage Capability of EPR Power Cables ...," CERN/EF/Beam Tech. 82-1, January 1982.

6. K. T. Gillen and R. L. Clough, "Dose Rate Effects for Material Aging Studies," SAND80-1146C, presented at Third International Conference on Radiation Processes, Tokyo, October 1980.

7. R. L. Clough and K. T. Gillen, "Radiation and Thermal Degradation of PE and PVC," SAND80-2149C, presented at Third International Conference on Radiation Processes, Tokyo, October 1980.

8. IEEE Standard 382-1980 (see e.g., Figure 7).

9. E. W. Bennet, ITT Suprenant Division, personal communication.

10. F. V. Thome, "Testing to Evaluate Synergistic Effects from LOCA Environments," SAND78-1718, April 1978.

11. C. Hosticka, et al., "Qualification of Cables to IEEE Standards," IEEE Transactions on Nuclear Science, NS-27, Vol. 1, February 1980.

12. IEEE Standard 383-1974, "Standard for Type Test of Class 1E Electrical Cables, Field Splices, and Connections for Nuclear Power Generating Stations."

13. M. Asaka, et al., "Radiation Resistance of Plastic Materials for Cables, Part 2," Fujikura Densen Giho, Vol. 48, 1973.

14. L. Corbelli and F. Tonioli, "Ethylene-Propylene Elastomers as Insulators in Electrical Technology," Kunststoffe, Vol. 30, Nr. 2/1977. (In German).

15. H. St. Onge, et al., "Research to Determine the Acceptable Emergency Operating Temperature of Extruded Dielectric Cable," EPRI Report EL 983, November 1978.

16. I. Kuriyama, et al., "Effect of Dose Rate on Degradation Behavior of Insulating Polymer Materials," IEEE Trans. on Electrical Insulation, EI-14, October 1878.

17. T. Seguchi, et al., "Dose Rate Effects on Chemical and Mechanical Properties," Takasaki Radiation Chemistry Research Establishment, JAERI, undated.

18. Y. Murata, et al., "Electrical Properties Under Radiation and Steam Environment," Sumitomo Electric Industries, EIM-79-91, NE-79-13*, 1979.

19. R. W. Sillars, "Electrical Insulating Materials," Peregrinus, London, p. 65 ff, (1973).

20. G. C. Derringer, et al., "Basic Study of the Aging Process," (Review Report), Batelle Institute, Columbus, November 1979.

21. S. Kronenberg, et al., "Gamma Ray Induced Charge Buildup in Insulators," Army Electronics Command, Fort Monmouth, AD 786655, September 1974.

22. O. M. Stuetzer, "Status Report on Reactor Cable Breakdown Correlation Study," Sandia Laboratories, unpublished, January 1983.

23. O. M. Stuetzer, "Test Sample Alignment for Creep Measurements," Sandia Laboratories, March 1983.

24. J. D. Ferry, "Viscoelastic Properties of Polymers," Wiley, New York (1970).

25. L. C. E. Struik, "Physical Aging in Amorphous Polymers ...," Elsevier, Amsterdam (1978).

26. K. T. Gillen, personal communication.

27. C. J. Aloisio and G. S. Brockway, "Thermomechanical Reliability of Plastics ...," International Conference on Plastics in Telecommunications 2, London, September 1978.

28. J. E. Reaugh, "Analysis of Insulator Cracking and Creep Shortout," Report of Activities under Sandia Contract, Science Applications, Inc., November 1982.

29. R. P. Wool and K. M. O'Connor, "A Theory of Crack Healing in Polymers," J. Appl. Physics, 52, 5923 (1981).

30. H. M. Gilroy, "Thermal Oxidative Cracking of Polyethylene Insulation," Bell Telephone Laboratories Report, 1974.

31. B. E. Klipec and S. M. Stephan, Samuel Moore Co., Ohio, 1976.

32. O. M. Stuetzer, "Electrical Insulators in a Reactor Accident Environment," NUREG/CR-1682, January 1981.

APPENDIX A

The complexity of failure assessment for cables in reactors is illustrated by the following parameter count.

A conservative (i.e., low count) estimate of independent parameters p is made. Tests or verification efforts depend on p and on the number n of samples taken or variations allowed for each parameter that influences (noticeably) cable failure, e.g., the breakdown voltage V_b.

The (simplified) test scenario has the cables first aged in a containment at temperature T_0, at radiation rate R_0, and humidity h_0 for a time t_0. This time t_0 may be 1 to 40 years in reality, and many months under accelerated aging. During t_0 we assume, for simplicity, no cable breakdown. After aging, accident conditions are assumed with enhanced parameters T_1, R_1, h_1 for a continuously increasing time t; where t will be the variable for measurements of $V_b(t)$.

A systematic list of parameters is presented in Table A-1. The list is self-explanatory. Some not immediately obvious points are:

A: Materials: "Additives" means both chemicals added before processing and flame retardants applied afterwards. The wire material is not only of mechanical importance, e.g., during bending, but also produces chemical effects (slow copper diffusion into the insulator enhances cracking.)

B: Geometry: The number of conductor strands has a first-order influence on creep effects. "Flaws" means both lacerations due to handling and geometric inconsistencies such as metal particulates or bubbles.

C: Circuit: The Load Impedance determines the current in the cable. "Frequency" alludes mainly to the fact that breakdown phenomena for alternating current are often quite different from those for direct current.

D: Aging: For experimentation, t_0 is the preselected time for accelerated aging. Under real conditions t_0 is the time at which the accident starts.

E: Accident: σ is the conductivity of the immediate cable environment, e.g., produced by condensation or reactor spray.

The list contains a number of simplifications (e.g., "flaws" covers a number of unrelated deficiencies causing quite different effects) and omissions (e.g., mutual heating of neighboring cables depends on some additional parameters such as

Table A-1 Cable test parameters (27)

Group	Parameter	Example
A. Materials:		
Insulator	Composition	n = 3
	Binders	2
	Additives	2
	Processing	1
Jacket	Composition	2
	Additives	1
	Processing	1
Wire	Material	2
B. Geometry and Forces	Wire Diameter	1
	Insul. Thickness	1
	Jacket Thickness	1
	# of Strands	2
	Bending Radius	4
	Applied Stress	2
	Flaws	1
C. Circuit	Voltage	1
	Load Impedance	2
	Frequency	2
	Off/On Percentage	2
D. Aging Exposure	Temperature T_0	3
	Rad. Rate R_0	3
	Humidity h_0	2
	Exp. Time t_0	1
E. Accident Parameters	Temperature T_1	2
	Rad. Rate R_1	2
	Humidity h_1	1
	Conduct. σ	2
Measurement Variable	Time t into accident	------

heat conductivity and separation). The compilation will serve its present purpose, however.

The number of parameters listed is p = 27. If each parameter had only one sample value n, we have, of course, defined only a single experiment. If each parameter is varied once, i.e., n = 2, the list leads to $n^p = 2^{27} \approx 134 \times 10^6$ different test configurations.

In the last column of Table A-1 an investigation is characterized that may be called "desirable" (3 materials for insulator, 2 for jacket, and many parameters neglected as indicated by n = 1). Even this list leads to almost 900,000 variations.

A severe aggravation is introduced by the fact that many of the above parameters are not well known; materials vary from batch to batch, some dimensions have wide tolerances, electrolytic conductivities vary with time, etc. To permit a statistical average, each test configuration must be represented several times - a factor of 3 or more to be applied to the above numbers.

DISTRIBUTION:

U.S. NRC Distribution Contractor
7300 Pearl Street
Bethesda, MD 20014
375 copies for RV

Ansaldo Impianti
Centro Sperimentale del Boschetto
Corso F.M. Perrone, 118
16161 Genova
ITALY
Attn: C. Bozzolo

Ansaldo Impianti
Via Gabriele D'Annunzio, 113
16121 Genova
ITALY
Attn: S. Grifoni

ASEA-ATOM
Department KRD
Box 53
S-721 04
Vasteras
SWEDEN
Attn: A. Kjellberg

ASEA-ATOM
Department TQD
Box 53
S-721 04
Vasteras
SWEDEN
Attn: T. Granberg

ASEA KABEL AB
P.O. Box 42 108
S-126 12
Stockholm
SWEDEN
Attn: B. Dellby

Atomic Energy of Canada, Ltd.
Chalk River Nuclear Laboratories
Chalk River, Ontario K0J 1J0
CANADA
Attn: G. F. Lynch

Atomic Energy of Canada, Ltd.
1600 Dorchester Boulevard West
Montreal, Quebec H3H 1P9
CANADA
Attn: S. Nish

Bhabha Atomic Research Centre
Health Physics Division
BARC
Bombay-85
INDIA
Attn: S. K. Mehta

British Nuclear Fuels Ltd.
Springfields Works
Salwick, Preston
Lancs
ENGLAND
Attn: W. G. Cunliff, Bldg 334

Brown Boveri Reaktor GMBH
Postfach 5143
D-6800 Mannheim 1
WEST GERMANY
Attn: R. Schemmel

Bundesanstalt fur Materialprufung
Unter den Eichen 87
D-1000 Berlin 45
WEST GERMANY
Attn: K. Wundrich

CEA/CEN-FAR
Departement de Surete Nucleaire
Service d'Analyse Fonctionnelle
B.P. 6
92260 Fontenay-aux-Roses
FRANCE
Attn: M. Le Meur
J. Henry

CERN
Laboratorie 1
CH-1211 Geneve 23
SWITZERLAND
Attn: H. Schonbacher

Canada Wire and Cable Limited
Power & Control Products Division
22 Commercial Road
Toronto, Ontario
CANADA M4G 1Z4
Attn: Z. S. Paniri

Commissariat a l'Energie Atomique
ORIS/LABRA
BP N° 21
91190 Gif-Sur-Yvette
FRANCE
Attn: G. Gaussens
J. Chenion
F. Carlin

Commissariat a l'Energie Atomique
CEN Cadarche DRE/STRE
BP N° 1
13115 Saint Paul Lez Durance
FRANCE
Attn: J. Campan

Conductores Monterrey, S. A.
P.O. Box 2039
Monterrey, N. L.
MEXICO
Attn: P. G. Murga

Electricite de France
Direction des Etudes et Recherches
1, Avenue du General de Gaulle
92141 CLAMART CEDEX
FRANCE
Attn: J. Roubault
L. Deschamps

Electricite de France
Direction des Etudes et Recherches
Les Renardieres
Boite Postale n° 1
77250 MORET SUR LORING
FRANCE
Attn: Ph. Roussarie
V. Deglon
J. Ribot

EURATOM
Commission of European Communities
C.E.C. J.R.C.
21020 Ispra (Varese)
ITALY
Attn: G. Mancini

FRAMATOME
Tour Fiat - Cedex 16
92084 Paris La Defense
FRANCE
Attn: G. Chauvin
E. Raimondo

Furukawa Electric Co., Ltd.
Hiratsuka Wire Works
1-9 Higashi Yawata - 5 Chome
Hiratsuka, Kanagawa Pref
JAPAN 254
Attn: E. Oda

Gesellschaft fur Reaktorsicherheit (GRS) mbH
Glockengasse 2
D-5000 Koln 1
WEST GERMANY
Attn: Library

Gesellschaft fur Reaktorsicherheit (GRS) mbH
Forschungsgelande
8046 Garching
WEST GERMANY
Attn: S. Gossner

Health & Safety Executive
Thames House North
Milbank
London SW1P 4QJ
ENGLAND
Attn: W. W. Ascroft-Hutton

ITT Cannon Electric Canada
Four Cannon Court
Whitby, Ontario L1N 5V8
CANADA
Attn: B. D. Vallillee

Imatran Voima Oy
Electrotechn. Department
P.O. Box 138
SF-00101 Helsinki 10
FINLAND
Attn: B. Regnell
K. Koskinen

Institute of Radiation Protection
Department of Reactor Safety
P.O. Box 268
00101 Helsinki 10
FINLAND
Attn: L. Reiman

Instituto de Desarrollo y Diseno
Ingar - Santa Fe
Avellaneda 3657
C.C. 34B
3000 Santa Fe
REPUBLICA ARGENTINA
Attn: N. Labath

Japan Atomic Energy Research Institute
Takasaki Radiation Chemistry
Research Establishment
Watanuki-machi
Takasaki, Gunma-ken
JAPAN
Attn: N. Tamura
K. Yoshida

Japan Atomic Energy Research Institute
Tokai-Mura
Naka-Gun
Ibaraki-Ken
319-11
JAPAN
Attn: Y. Koizumi

Japan Atomic Energy Research Institute
Osaka Laboratory for Radiation Chemistry
25-1 Mii-Minami machi,
Neyagawa-shi
Osaka 572
JAPAN
Attn: Y. Nakase

Kraftwerk Union AG
Department R361
Hammerbacherstrasse 12 + 14
D-8524 Erlangen
WEST GERMANY
Attn: I. Terry

Kraftwerk Union AG
Section R541
Postfach: 1240
D-8757 Karlstein
WEST GERMANY
Attn: W. Siegler

Kraftwerk Union AG
Hammerbacherstrasse 12 + 14
Postfach: 3220
D-8520 Erlangen
WEST GERMANY
Attn: W. Morell

Motor Columbus
Parkstrasse 27
CH-5401
Baden
SWITZERLAND
Attn: H. Fuchs

NOK AG Baden
Beznau Nuclear Power Plant
CH-5312 Doettingen
SWITZERLAND
Attn: O. Tatti

Norsk Kabelfabrik
3000 Drammen
NORWAY
Attn: C. T. Jacobsen

Nuclear Power Engineering Test Center
6-2, Toranomon, 3-Chome
Minato-ku
No. 2 Akiyana Building
Tokyo 105
JAPAN
Attn: S. Maeda

Ontario Hydro
700 University Avenue
Toronto, Ontario M5G 1X6
CANADA
Attn: R. Wong
B. Kukreti

Oy Stromberg Ab
Helsinki Works
Box 118
FI-00101 Helsinki 10
FINLAND
Attn: P. Paloniemi

Rheinisch-Westfallscher
Technischer Uberwachunge-Vereln e.V.
Postfach 10 32 61
D-4300 Essen 1
WEST GERMANY
Attn: R. Sartori

Sydkraft
Southern Sweden Power Supply
21701 Malmo
SWEDEN
Attn: O. Grondalen

UKAEA
Materials Development Division
Building 47
AERE Harwell
OXON OX11 ORA
ENGLAND
Attn: D. C. Phillips

United Kingdom Atomic Energy Authority
Safety & Reliability Directorate
Wigshaw Lane
Culcheth
Warrington WA3 4NE
ENGLAND
Attn: M. A. H. G. Alderson

Waseda University
Department of Electrical Engineering
4-1 Ohkubo-3, Shinjuku-ku
Tokyo
JAPAN
Attn: K. Yahagi

1200 G. Yonas
1234 J. Chang/G. J. Lockwood
1800 R. L. Schwoebel
1810 R. G. Kepler
1811 L. A. Harrah
1811 R. L. Clough
1812 K. T. Gillen
1813 J. G. Curro
1815 R. T. Johnson
2155 J. E. Gover
2155 G. J. Simmons
2155 O. M. Stuetzer (10)
2321 D. McKeon
2341 M. B. Murphy
5200 W. C. Myre
6200 V. L. Dugan
6300 R. W. Lynch
6400 A. W. Snyder
6410 J. W. Hickman
6420 J. V. Walker
6432 D. D. Carlson
6440 D. A. Dahlgren
6442 W. A. Von Riesemann
6444 S. L. Thompson
6445 B. E. Bader
6445 L. D. Bustard
6445 C. M. Craft
6446 L. L. Bonzon (20)
6446 W. H. Buckalew
6446 J. W. Grossman
6446 D. B. Hente
6446 F. V. Thome
6446 F. J. Wyant
6447 D. L. Berry
6449 K. D. Bergeron
6450 J. A. Reuscher
6450A J. Bryson
6452 M. Aker/J. S. Philbin
7550 F. W. Neilson
7551 B. D. Hansche
7551 D. G. Sample
8424 M. A. Pound
3141-1 C. M. Ostrander (5)
3151 W. L. Garner (3)

NRC FORM 335 (2-83) U.S. NUCLEAR REGULATORY COMMISSION

BIBLIOGRAPHIC DATA SHEET

1 REPORT NUMBER (Assigned by TIDC and Vol. No. if any)
NUREG/CR-3263
SAND83-2622

2 Leave blank

3 TITLE AND SUBTITLE
Status Report: Correlation of Electrical Cable Failure with Mechanical Degradation

4 RECIPIENT'S ACCESSION NUMBER

5 DATE REPORT COMPLETED
MONTH: March YEAR: 1984

6 AUTHOR(S)
Otmar Stuetzer

7 DATE REPORT ISSUED
MONTH: April YEAR: 1984

8 PERFORMING ORGANIZATION NAME AND MAILING ADDRESS (Include Zip Code)
Sandia National Laboratories
Albuquerque, New Mexico 87185

9 PROJECT/TASK/WORK UNIT NUMBER

10 FIN NUMBER
NRC FIN No. A-1051

11 SPONSORING ORGANIZATION NAME AND MAILING ADDRESS (Include Zip Code)
Office of Nuclear Regulatory Research
U.S. Nuclear Regulatory Commission
Washington, DC 20555

12a TYPE OF REPORT

12b PERIOD COVERED (Inclusive dates)

13 SUPPLEMENTARY NOTES

14 ABSTRACT (200 words or less)

An attempt is being made to assess complete electrical failure of signal and low-power cables typically used in nuclear power plant containments and to correlate failure modes with the mechanical deterioration of the elastomeric cable material. Work over the past 24 months, although limited to one cable configuration, has identified creep shortout and insulator cracking, both aggravated by mechanical stresses, as the phenomena most likely to cause electrical breakdown. Comprehensive tests have been run for six months and are continuing. Preliminary conclusions can be drawn and are reported.

15a KEY WORDS AND DOCUMENT ANALYSIS

15b DESCRIPTORS

16 AVAILABILITY STATEMENT
Unlimited

17 SECURITY CLASSIFICATION (This report)
Unclassified

18 NUMBER OF PAGES
90

19 SECURITY CLASSIFICATION (This page)
Unclassified

20 PRICE
$

☆U.S. GOVERNMENT PRINTING OFFICE:1984—776-027 / 4303

ORG.	BLDG.	NAME	REC'D BY*	ORG.	BLDG.	NAME	REC'D BY*

120555056729 1 IANIRV
US NRC
NRR-DIV OF ENGINEERING
BRANCH CHIEF
EQUIPMENT QUALIFICATION BR
P-234
WASHINGTON DC 20555

Sandia National Laboratories